McGill Rocket Team: Project Ariel
Base11 Phase 1 Preliminary Design Report
McGill University, Montreal, Quebec, Canada, H3A 0E9

Daniil Lisus*[5], Liem Dam-Quang[†1], Camille Richer[‡2], Julien Otis-Laperriere[1], Matthew Saathoff[1], Anthony Laye[3], Juan Li[1], Julian Zhang[1], Charles Renshaw Whitman[1], Joel Jean-Philyppe[1], Sarim Malik[§5], Angel Miao[5], Chris DiSalle[5], Natasha Laye[5], Serge Krikorian[5], Joel Sabot[4], George Wang[4], Madison Santos[4], Anthony Ubah[3], and Zijing Yan[2]

[1]*Propulsion Group*
[2]*Aerostructures Group*
[3]*Avionics Group*
[4]*Payload Group*
[5]*Business Group*

This document provides the preliminary design of *Project Ariel*: a single-stage liquid engine rocket with a target apogee of greater than 100km altitude, the Karman line. *Project Ariel* will feature McGill's first ever student built liquid engine *Prospero*. Every system will be largely researched, designed and manufactured by students.

Contents

---

*CEO
[†]Chief Engineer
[‡]Chief Safety Officer
[§]Business Development Director

I. Introduction

A. Team Structure

The structure of the McGill Rocket Team for the Base11 challenge is as distributive as possible. With the size of the Base11 team growing above 50 people, and around 100 other students who are not directly involved in Base11 yet, there are ideally plenty of contributors to the project. This means that the leads can focus on overall systems integration and management rather than having to do everything themselves.

The current structure has 5 different subteams and 3 main people responsible for overarching continuity. The subteams are:

1) *Management*: This subteam deals with fund-raising, social events, team brand, promotional materials and general logistics. It is led by the Business Development Director(s).

2) *Aerostructures*: This subteam deals with the physical structural components of the rocket. This includes the body tubes, nosecone, fins, couplers, internal structures, decoupling mechanism and recovery harness. It develops the Internal Structures and Aerostructures subsystems as defined in the SE Diagrams. It is lead by the Aerostructures Lead(s).

3) *Avionics*: This subteam is primarily responsible for the flight computer and ground station, however assists in all electronics across the project. It develops the Flight Computer subsystem as defined in the SE Diagrams. It is lead by the Avionics Lead(s).

4) *Propulsion*: This subteam is responsible for the propulsion system of the rocket, including any testing facilities and on-pad filling procedures. It develops the Propulsion subsystem as defined in the SE Diagrams. It is lead by the Propulsion Lead(s).

5) *Payload*: This subteam is responsible for the payload aboard the rocket. It develops the Payload subsystem as defined in the SE Diagrams. It is lead by the Payload Lead(s).

Figure 1   MRT Team Structure

Additionally, there are 3 supporting figures that oversee the project as a whole:

1) *The Captain/CEO*: Responsible for ensuring the project is on target with respect to all subteams.

2) *The Chief Engineer*: Responsible for ensuring that all technical systems and subsystems are on target and well integrated.

3) *The Chief Safety Officer*: Responsible for the safe conduct and operation of all members and systems, at every point of the project from training to launch day.

The other members will initially be "SUBTEAM Member" (ie. Propulsion Member), but will have titles defined based on the sub-subsystem they will be working on. This is to ensure that everyone feels responsible for a specific sub-project

and can be recognized based on what their efforts are going into.

Note that an official sorting of members has not yet been done, so apart from the mandatory roles everyone is still listed as a general member. This will be changed as soon as sub-subsystems are finalized.

B. Management Strategy

The team's goal is to integrate as many members as possible, which means trying to reduce the hierarchical nature of the team so that those who want to be proactive, can be proactive on any level they want. However, for the sake of productivity and deliverables, there need to be key people responsible for overseeing that projects get completed. This means that there exists a responsibility hierarchy, without a decision-making one. Every member of a project should understand where the project is going, what is left to do and why certain key decision were made. This approach is about team culture, and we have been working on making sure that all information is as transparent as possible, and all members are invited to be proactive and contribute.

C. Stakeholders

There are 4 main stakeholders to the project, 2 of which represent a group of stakeholders.

1) *Students*: The team is, above all else, meant as a means for students to gain hands on experience and to develop their passion for and technical skills in the field of aerospace. The team has a responsibility to provide those opportunities to its members

2) *Base11*: The organization is a stakeholder in every project that is participating, and expects the team to be responsible, safe and to do the necessary work to ensure a successful result. The team has an obligation to submit all necessary materials on time and keep a clear line of communication with the organization.

3) *McGill University*: The university includes smaller stakeholders such as faculty advisors, safety committees, faculty and other administrative groups. The team has a responsibility to represent the university in a respectful manner and abide by the rules that the university sets out. As most work is done on campus, this stakeholder has a lot of power over facilities and manufacturing.

4) *Sponsors*: Sponsors are what allow the project to progress and to reach completion. In-kind and cash sponsorships make the whole operation possible, and thus they are an important stakeholder to be accountable to. The team is responsible for holding up its end of the sponsorship deals such as social media featuring, displaying logos on apparel and other specifics.

The team relies on all these stakeholders in order to successfully complete the project, however the project cannot be complete without the team being accountable about their responsibilities to each stakeholder in turn.

D. Systems Engineering Approach

Project Ariel will have a target altitude an order of magnitude greater than anything the McGill Rocket Team has attempted before. To take on the challenge of our first ever space shot and ensure the final vehicle meets all requirements, the team has taken a top-down designing approach.
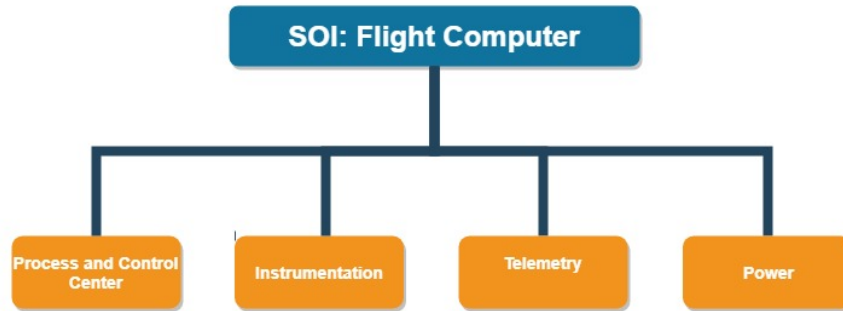
Figure 2   SOI: Flight Computer Decomposition Diagram

For this report, our aim was to design the rocket while staying as solution free as possible. This means that we tried to decompose the rocket into as many layers of subsystems as possible, without implying how those subsystems will be built or what they will look like. An example of this can be seen in Figure 2, where the Flight Computer aboard the rocket is decomposed into one level, without implying any solutions. The full decomposition into another layer can be seen in our auxiliary files. The intent behind this is to ensure that all aspects of the project are defined before we fully dive into design, as well as to help maintain coherency within the project across the years. Lastly, every member of the team should be able to look at the diagrams and understand the layout of the rocket, without having to get into the specifics of what RF interference is or what an engine plumbing diagram looks like.

The next step in the process, will be to add one more layer to the diagram with specific physical subsystems that will achieve the necessary logical components defined at the higher level. This will be a key step, as after this we will be able to fully sort the individual projects that need to be completed, what inputs/outputs those systems need to take/produce and what requirements they must satisfy. The last step will be for the groups working on each individual physical subsystem to break it down even further into physical components at the lowest level, transferring requirements onto them and describing how they will be produced.

When this full SE diagram is completed, we will have built our rocket without having made any physical components. The next step will be to bring all systems to completion and integrate them together by going back up the chart to assembled each subassembly.

Although the focus of the team has been the Rocket as an SOI, the Ground Operations system will similarly be detailed and brought to completion by the same approach. The overall system that is being designed is termed the Ariel Space Launch System (ASLS). The current diagrams contain 3 layers each, with the SOI's being the ASLS, and each of the 4 Rocket subsystems. The key functional and performance requirements identified for the ASLS, Rocket, Ground Operations and each of the Rocket subsystems are included throughout the diagrams.

II. Design

A. Description of Overall System Architecture

A top level overview of the System Architecture can be seen in our SE Diagrams, with the SOI: Ariel Space Launch System. The overarching system that is being designed is the Ariel Space Launch System, which has two major sub-systems: the Rocket and Ground Operations. As can be seen in the SE Diagram for the Ariel Space Launch System SOI, both the Rocket and Ground Operations are composed of 5 sub-systems, adding up to a total of 10 critical top-level subsystems. Together, these two layers of detailing compose the main System Architecture for Project Ariel.

1. Systems Summary
   1) Rocket System
      1) *Propulsion*: This system provides the propulsion for the Rocket, allowing it to reach the target altitude. It poses one of the greatest risks involved in both developing the project and during launch day. It must

interface with the Fuelling System to allow propellant to be loaded and be remotely caused to begin producing propulsion. The main requirement on the design of the system is that it must be single-stage and bi-liquid propelled. Lastly, this system but interface with the Internal Structures.

2) *Aerostructures*: This system provides the physical structure for the Rocket and sustains all externally applied thermal and mechanical loads. It deals with all components that come together to form the outside of the Rocket, and deals with how those components interface with one another. Lastly, this system must interface with the Launch Pad during launch operations and be assembellable at the Assembly Pad.

3) *Internal Structures*: This system provides the enternal frame for all sub-systems housed inside the Aerostructures sub-system. This system also sustains all internal thermal and mechanical loads and ensures that the sub-systems contained within Aerostructures are protected from thermal and mechanical loads if need be. Additionally, the recovery hardware is contained within this subsystem. Lastly, this system must interface with all other Rocket sub-systems, as it is connected to all of them.

4) *Flight Computer*: This system provides all telemetry and communication for the Rocket. It must interface with the Ground Computer at all times during flight. It does not include all electronics aboard the rocket, but does the majority of data gathering and processing, as well as activates energetics for various events in-flight. Lastly, it must interface with the Internal Structures.

5) *Payload*: This system contains the mission of the flight. Depending on this mission, the Payload must interface with the Internal Structures and any other system that may affect it.

2) Ground Operations System

1) *Assembly Pad*: The Assembly Pad system functions to ensure a fluid and timely assembly of the Rocket. It must interact with all Rocket sub-systems to ensure full assembly. All systems must be SAFED whenever on or around the Assembly Pad. This system does not include the Payload assembly, however can be directly interfaced with the Payload Operations system.

2) *Fuelling System*: This system provides all active and supporting equipment involved in delivering oxidizer and fuel to the rocket engine. It directly interacts with the Propulsion System inside the Rocket, and is required to have extensive safety fail-safes as personnel will be in proximity for large parts of the filling.

3) *Launch Pad*: This system is responsible for providing all interface to Rocket subsystems during Fuelling System operations and final ARMING procedures. This system is also responsible for providing stability to the Rocket during take-off.

4) *Ground Computer*: The Ground Computer is responsible for all data reception and processing from the Flight Computer. It must be operational during the whole launch procedure, from the moment the Flight Computer is turned on. This system includes signal reception devices and computers to process, store and display that data.

5) *Payload Operations*: This system is required to provide all necessary equipment and features to handle pre and post flight Payload needs. This can involve a direct interface with the Assembly Pad, Launch Pad and other subsystems.

2. System Integration

System integration is extremely critical when designing large projects with multiple sub-systems. If systems integration is left till the end, many problems may arise and prevent the project from being completed in time. To combat this, the team is undertaking a top-down systems engineering approach. This means that every sub-system must be derived from a higher system, ensuring that redundancy is lowered. With the goals and requirements for each higher level system clearly laid out, any changes in the subsystem simply need to comply with the higher system. This means that changing one will should not have to be validated against the whole rocket, but should ideally only be validated as far whether that change still falls within the expected behaviour of the sub-system that component is a part of.

B. Mission Concept of Operations Overview

The overall mission can be described as "safely setup, deploy and recover Ariel to an apogee of over 100km". Here, Ariel refers to the entirely of the assembled rocket implying that everything that goes up must be recovered. Additionally,

the mission makes an emphasis on the safety of all operations, as that is the largest concern for involved members and staff. The mission concept of operations will be explained using second layer subsystems (immediately below Rocket and Ground Operations), and will go through 3 main phases as implied by the statement:

1) Setup

2) Deployment

3) Recovery

1. Phase 1: Setup
　　1) **Sub-phase 1: Assembly -** Setup begins at the Assembly Pad, where the rocket and all systems are assembled. Nominal procedure is a timely assembly which follows every step of the checklist. Safety concerns are minimal, energetics are inside the rocket but all energetic systems must be SAFED.
　　Trigger: Assembly Checklist Completion - Once the assembly checklist has been completed, the Assembly sub-phase transitions to Installation.

　　2) **Sub-phase 2: Installation -** Installation involves transporting the rocket to the Launch Pad, where it is installed onto the Launch Pad. Nominal procedure is a bump-free transportation and followed checklist for installation onto Launch Pad. Installation concludes with turning on the telemetry circuits of the Flight Computer to verify data transmission on the Ground Computer. Safety concerns are minimal, energetics are inside the rocket but all energetic systems must be SAFED.
　　Trigger - Installation Checklist Completion: Once the installation checklist has been completed, the Installation sub-phase transitions to Fuelling.

　　3) **Sub-phase 3: Fuelling -** Fuelling is achieved by the Fuelling System and happens on the Launch Pad, where the rocket is filled with oxidizer and fuel. Nominal procedure is a safe connect, control and disconnect of the fuelling system and followed checklist for fuelling. Safety concerns are large, oxidizer and fuel handling can be extremely dangerous and the plumbing must be able to accommodate emergency shut off, depressurization and other failure criteria, however all energetic systems must be SAFED.
　　Trigger: Fuelling Complete - Once the fuelling has been completed, the Fuelling sub-phase transitions to Arming.

　　4) **Sub-phase 4: Arming -** Arming is achieved by engaging all systems of the Flight Computer. Nominal procedures are a successful continuity check and continual transmission of data to the Ground Computer. Safety concerns are large, the rocket is fully fuelled and energetic systems are turned on and verified through a continuity check and through the Flight Computer, all systems are set to ARMED.
　　Trigger: Personnel cleared - Once the circuit is armed, all personnel must clear to a safe distance, the Arming sub-phase transitions to Deployment phase.

2. Phase 2: Deployment
　　1) **Sub-phase 5: Ignition -** Ignition occurs on the Launch Pad, either through the Ground Computer or by some other external means after authorization is given to launch. Nominal procedure is an expected ignition event and functioning Propulsion System. Safety concerns are large, the motor is igniting for the first time. All personnel must be at an appropriate distance away.
　　Trigger: LAUNCH button is pressed - Once the authorization is given, the LAUNCH button is pressed and the Rocket transitions from Ignition to Liftoff.

　　2) **Sub-phase 6: Liftoff -** Liftoff occurs on the Launch Pad, up until the Rocket has reached sufficient speed. Nominal procedure is an expected motor burn and rocket stability on the Launch Pad as it is accelerating. Safety concerns are large since the rocket has not yet reached stable flight and is close to the ground.
　　Trigger - Sufficient liftoff velocity is reached Once the Propulsion System has generated enough Rocket velocity for the Rocket to leave the Launch Pad, the Liftoff sub-phase transitions to the Powered Ascent Phase.

　　3) **Sub-phase 7: Powered Ascent -** Powered Ascent is the phase of Rocket ascent during which the Propulsion System is propelling the Rocket. Nominal procedure is a controlled climb and steady motor burn. The Airframe and Internal Structures must sustain all external and internal loads respectively during Powered Ascent. The

Flight Computer should be transmitting to the Ground Computer at all times. Safety concerns are large, since a catastrophic failure could lead to rapid unscheduled disassembly over personnel.

Trigger: Propulsion System shut-off - Once the Propulsion System shuts off, the Rocket transitions from the Powered Ascent to Coasting sub-phases.

4) **Sub-phase 8: Coasting -** Coasting occurs when the Rocket is gaining altitude, but the Propulsion System is no longer providing thrust. Nominal procedures involve a continual straight ascent, with all external and internal conditions maintained by the Airframe and Internal Structures. The Flight Computer should be transmitting to the Ground Computer at all times. Safety concerns are low, the rocket has most likely passed Max Q and the worst structural loads.

Trigger: Apogee reached - Once the Rocket reaches its apogee, it will transition from Coasting sub-phase to the Recovery phase.

3. Phase 3: Recovery

1) **Sub-phase 9: Controlled Descent -** Controlled Descent happens as soon as rocket reaches apogee, and the first parachute is deployed and includes all deployment events. Nominal procedure is clean separation and deployment for every parachute phase. Safety concerns are minimal as the rocket is likely far away from any personnel, however system failure chance is high due to potential of failure to separate and deploy any parachute stage.

Trigger: Rocket touchdown - Once all parachutes have been deployed and the rocket descends to the ground, the Controlled Descent will transition to Ground Recovery.

2) **Sub-phase 10: Ground Recovery -** A team of recovery members must recover the rocket based on Ground Computer information provided about the point of touchdown. The Rocket is then transported back to base camp for examination. Payload Operations may be involved with the post-processing of the Payload. This is the last sub-phase for the launch event.
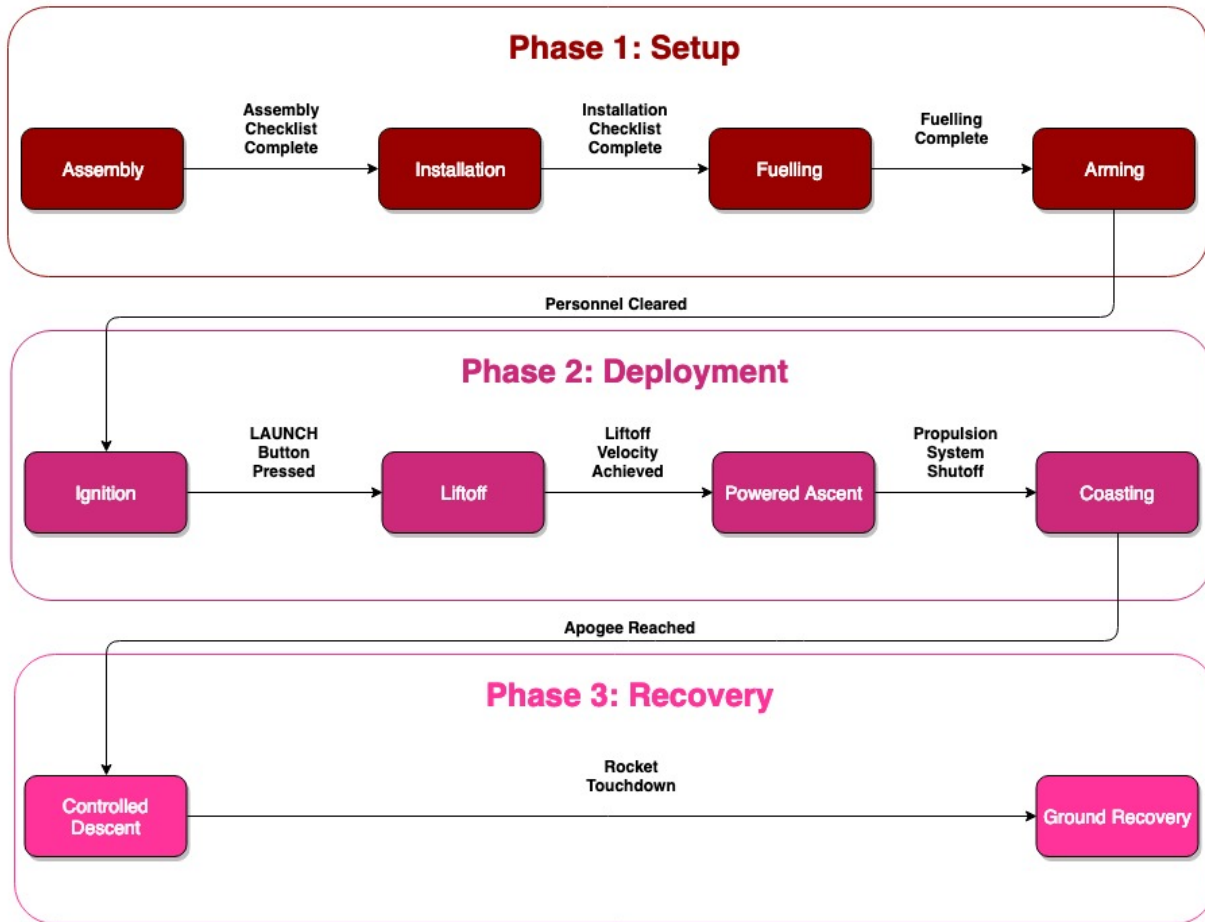
Figure 3   Mission Concept of Operations Overview

C. Mission Analysis

As mentioned above, the overall mission is to safely launch Ariel up to an apogee of 100km, and to safely recover the rocket in its entirety. Mission requirements can be derived both from system architecture and concept of operations, as both constrain rocket design. At the level of the rocket system, the following requirements apply:

1) 100km apogee
2) Liquid bi-propellant engine
3) Single stage
4) Non-zero payload capacity
5) Fully recoverable

Accordingly, and as explained at length in section II.A.1, each rocket subsystem implements the following:

1) *Propulsion*: 100km apogee, liquid bi-propellant engine, single stage.
2) *Aerostructures*: 100 km apogee, single stage, fully recoverable.
3) *Internal Structures*: 100km apogee, non-zero payload capacity, fully recoverable.
4) *Flight Computer*: 100km apogee, fully recoverable.
5) *Payload*: 100km apogee, non-zero payload capacity.

Of the above subsystems, the Team chose to begin by designing the Propulsion system, as it is the system that most constrains the rest of the rocket: it's much easier to design a rocket around an engine, than to design an engine around

a rocket. This is especially true for this project, as the Team is a student group with limited financial, human, and infrastructural resources. As a result, identifying and designing a *feasible* engine first was a priority, as otherwise the whole Ariel project could collapse if the Propulsion team couldn't design an engine to match and ambitious rocket. Of course, engine design was iterative: an initial "guess" based on available literature was slowly tuned until it allowed all the subsystems to meet their requirements. Then, a first set of requirements for the engine was brought forth:

1) The engine should generate 2100 m/s of ΔV or more;
2) The engine should operate on liquid oxygen and a well-known, safe, and easily available fuel;
3) The combustion pressure should remain within *reasonable* limits, to allow for an injector pressure drop of 25-40%;
4) The engine must be pressure-fed, as turbopump design is beyond the capability of the team;
5) The oxidizer flow rate must be below 3kg/s, as anything higher would significantly increase test-site cost and complexity.

From the above, the design space of the engine was significantly constrained. Req. 1. constrained the mass ratio of the rocket and the exhaust velocity, as $\Delta V = v_e x h ln(\frac{m_full}{m_empty})$, assuming a constant exhaust velocity, which is fair at this stage. Req. 2 narrowed the range of potential fuels: common fuels such as hydrogen were deemed unsafe, while unsaturated hydrocarbons such as ethylene or propylene were ruled out based on their rarity in industry and literature. Given the resources of the team, RP-1 seemed inaccessible, leaving the Alkane family on the table. According to [1], methane and propane were two very energy dense fuels, and so the Team settled on running simulations with both. Meanwhile, Req. 3 and 4 forced the combustion chamber to run below 1000 psi, based on pressure vessel design requirements: as propellant feed pressure and pressurant mass both increase, tank weights follow suit and so the gains in efficiency in running a high-pressure combustion chamber are quickly offset. As a result, a combustion chamber pressure range of 500-1000psi was selected, and thus an on-board propellant storage pressure range of 750psi to 1500psi emerged. Finally, Req. 5 coupled with the combustion pressure limit capped the maximum thrust the engine could produce. As a result, we looked for weight-saving solutions, and the idea of insulating our liquid oxygen with a sub-cooled propane layer emerged, as propane would act as a buffer between environmental heat and the oxygen, without freezing due to the cryogenic temperatures. Thus, the initial engine had the following parameter:

1) Chamber pressure = 500 psi
2) Propellant: propane
3) O/F ratio: 2.6 (from ProPEP simulations)
4) Combustion temperature: 3150 (from literature)°C
5) Maximum oxidizer flowrate: 3kg/s
6) Nozzle inlet radius: 2.75 inches
7) Design Thrust: 10 kN

Note that the thrust and nozzle values were both design values, meaning that they were educated guesses as to what the final engine would resemble. A simple 1D flight simulator was created in Python to simulate the "flight" of this prototype engine, if it was attached to simple circular cross section with an arbitrary dry mass moving upwards. This allowed the team to iteratively search for the mass fractions that allowed the engine to produce enough ΔV to meet its requirements. Once the engine parameters were tweaked slightly to ride closer to their respective maximums, another Python script was written to determine the dry mass and length of the rocket as a function of the loaded propellant mass and rocket internal diameter. To determine the weight of the airframe, a conservative composite layup was used to estimate airframe linear weight. This exercise allowed the Team to decide on a propellant and pressurant tank design: composite overwrapped pressure vessels would need to be used (see section II.F.3 for details), else an entire engine re-design was in order, which would have resulted in an enormous rocket beyond the financial means of the Team. Using the same naive flight simulator, different propellant masses and diameters were simulated, resulting in the a series of estimated apogees, shown in figures 4, 5 and 6. Note that helium was used as a pressurant, stored at 5000 psi.

Optimal Setup:
D = 10.5"
Apogee = 105121.3 km
ΔV = 1970 m/s
Isp = 281.2 s
Dry Mass = 146.3 kg
Propellant Mass = 160 kg

Figure 4   Plot of rocket apogee as a function of diameter with propellant mass of 160kg

Optimal Setup:
D = 11.75"
Apogee = 139183.5 km
ΔV = 2206 m/s
Isp = 282.8 s
Dry Mass = 154.2 kg
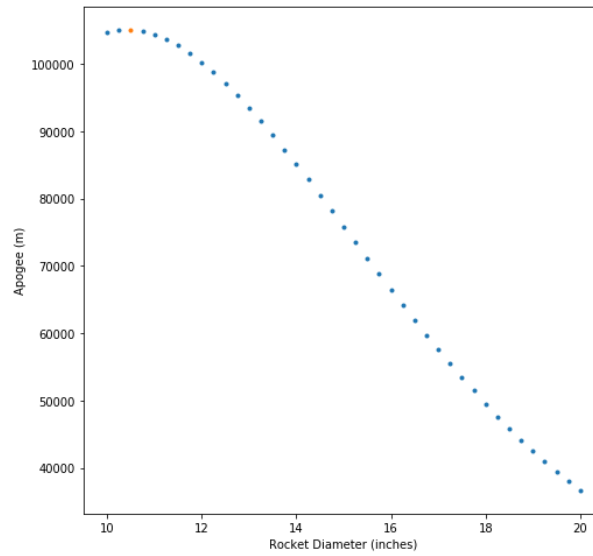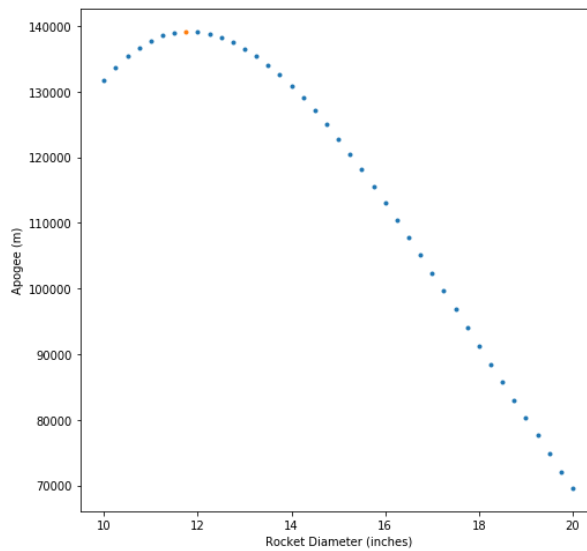Propellant Mass = 200 kg

Figure 5   Plot of rocket apogee as a function of diameter with propellant mass of 200kg
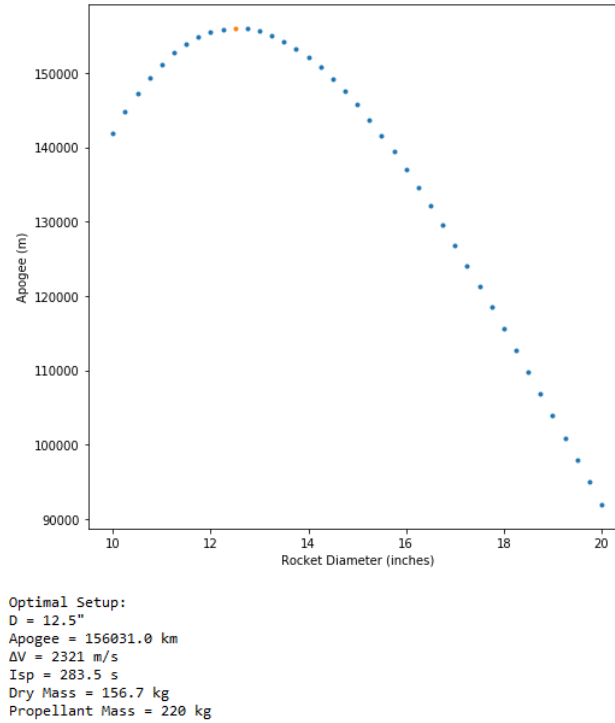
Figure 6   Plot of rocket apogee as a function of diameter with propellant mass of 220kg

From this, more accurate and complete models of the rocket were built in OpenRocket of rockets with 200kg and 220kg of propellant onboard. Note that the "optimal setup" identified by the 1D simulator was not selected, mostly because it produced rockets that were ridiculously long (10+ m) compared to their width; in furth analysis, these would have been likely to crumple under bending moments. OpenRocket was used for more accurate flight simulations, which include a full 3D aerodynamics model with in-depth drag analysis. The result was a 20% decrease in apogee across the board, leaving only the 14" diameter rocket with 220kg of propellant to reach above the desired apogee floor of 100km. In simulations, this model performed nominally, with the most important flight results tabulated below in Table 1.

Specification	Value	Unit
Airframe Length	8.5	m
Airframe Diameter	14.0	in
Liftoff Mass	414.3	kg
Peak Thrust	13.0	kN
Max Mach Number	4.76	Mach
Predicted Apogee	104	km
Thrust/Weight Ratio	3.075	-
Rail Departure Speed	27.5	m/s

Table 1   Key Technical Specifications

D. Requirements

The system requirements were taken from those provided by Base11, and our own were added based on necessity. As we have not yet detailed lower level sub-systems, the list of requirements is very high-level. Most of the requirements were derived from the teams past experience with rocketry. The non-Base11 mandated requirements are visible in the SE diagrams, as that is the method through which lower systems, which have to obey those requirements, will be

constructed.

Ultimately, there will exist a requirements document which lists every requirement for every system, which are split into functional, performance and safety requirements. Lastly, there will be a requirements trace-ability diagram which will allow to see the connection between lower and higher level requirements.

E. Mass Budget

The most significant consideration for our mass budget is the mass of the propulsive and structural systems. These are the factors which contribute most strongly to the system mass, with the exception of the propellant mass which is effectively determined by the dry system mass in conjunction with the rocket equation

$$m_{fuel} = m_{dry} \left[exp \left(\frac{\Delta V}{V_e} \right) - 1 \right]$$

Our mission goal and system architecture place firm constraints on ΔV and V_e so that the fuel mass becomes a fixed function of a specified dry mass. Our goal in design is thus to select the components which perform the necessary functions while maintaining a minimal weight; a challenge familiar to all rocketeers!

System	Mass (kg)
LOx Tank	27.94
Fuel Tank	18.17
Helium Tank	9.04
Combustion Chamber	6.2
Nozzle	0.5
Plumbing Allowance	35
Propellants	220
Tank Fixtures	15
Avionics	4
Payload	1
Recovery	15
Airframe and Structures	62.41
TOTAL	414.3

Table 2 Approximate tabulation of mass budget

F. Propellant Selection and Propulsion Design

1. Propellant Selection

In determining the propellants to be used, the primary factor under consideration was energy density. To this end, we have determined to use Liquid Oxygen (LOX) as our oxidizer, and propane (C_3H_8) as our fuel. The selection of LOX was straightforward: there aren't many great oxidizers, and it is a high-performance and relatively safe option. Despite the difficulty involved with handling cryogenic fluids, the high density propellant storage afforded by use of liquid oxygen outweighs the associated disadvantages. For propane, it was selected because when cooled to low temperatures yields a high bulk energy density of 1014 kg/m^3[1]. Another advantage of propane was that it could serve as an insulator for oxygen if concentric propellant tanks were designed. Unfortunately, the complexity associated with manufacturing concentric COPV tanks has made this option unfeasible as of writing. For the time being, propane is kept as all engine analysis was previously done using propane. Other propellants considered are methane (or liquid natural gas), RP1 (kerosene), and ethanol.

2. Combustion Chamber and Nozzle

In determining the preliminary dimensions of the combustion chamber, a primitive heat transfer model (steady-state, 1-D, convection on both sides) was applied to the section wall. Far from the ends of the chamber, the temperature in the wall is approximated as

$$T(x) = (1 - \frac{h_L x}{k}) \frac{T_R h_R - T_L h_L (Bi_R - 1)}{h_R - h_L (Bi_R - 1)} + \frac{h_L T_L}{k} x$$

with x between 0 and L describing distance from the 'cold' wall. Further, $Bi_R = h_R L/k$. From this relation, we can determine that, for preliminary values of k, T_L and T_R, assuming $h_L \approx 2h_R$, the chamber thickness is not limited by thermal, but structural, considerations. From this, we wish to have a chamber wall roughly 0.04" thick.

This being said, the effective implementation of cooling systems relies on complex geometry to direct propellant flow. As such we have determined it desirable to undertake to 3D-Print our combustion chamber along with an integral cooling sleeve. The cooling sleeve will allow us to direct cryogenic propellant flow in order to cool the engine. One company capable of doing this is FusiA Groupe, who we intend to contact once more final designs are completed. The material from which the chamber is to be printed has not yet been determined, though the above considerations provide preliminary characteristics.

In order to determine an optimal nozzle geometry, the quasi 1-D isentropic equations of flow were solved for a fixed thrust, chamber pressure, chamber temperature, design altitude, and propellant selection. To find the chemical and thermodynamic properties of the exhaust, ProPEP3 was used. With these parameters, the exhaust velocity and total propellant mass flow are given by:

$$v_e = \sqrt{\frac{2RT_c\gamma}{M(\gamma - 1)} \left(1 - \left(\frac{P_{atm}}{P_c}\right)^{\frac{\gamma-1}{\gamma}}\right)}$$

$$\dot{m} = \frac{F}{v_e}$$

Next, the conditions at the throat are given by:

$$P_t = P_c \left(\frac{2}{\gamma + 1}\right)^{\frac{\gamma}{\gamma-1}}$$

$$T_t = T_c \frac{2}{\gamma + 1}$$

$$\rho_t = T_c \frac{M}{RT_t}$$

$$v_t = \gamma \frac{P_t}{\rho_t}$$

From these the optimal throat radius can be found using:

$$r_t = \sqrt{\frac{\dot{m}}{\pi \rho_t v_t}}$$

Next, the exhaust conditions at the exit can be determined:

$$T_e = T_c \left(\frac{p_{atm}}{p_c}\right)^{\frac{\gamma-1}{\gamma}}$$

$$\rho_e = P_{atm} \frac{M}{RT_e}$$

$$M_e = \frac{v_e}{\sqrt{\gamma p_{atm} \rho_e}}$$

Finally, the optimal area ratio can be determined using:

$$\epsilon = \frac{A}{A^*} = \frac{1}{M_e}\left(\frac{\gamma+1}{2}\right)^{-\frac{\gamma+1}{2(\gamma-1)}}\left(1+\frac{\gamma-1}{2}M_e^2\right)^{\frac{\gamma+1}{2(\gamma-1)}}$$

To further refine these parameters, a Python tool was made which simulates the flight of a simplified rocket model. By running simulations with small variations in the design parameters, the design parameters can be optimized.From these parameters, the geometry of the nozzle is determined using the Rao Optimization Method, which, given an area ratio and nozzle length, uniquely determines the contour for which the ejected flow will produce maximum thrust. [2]

3. COPV Design

For the COPVs used on board this rocket, which will be used for the LOX tank, the propellant tank and the Helium tank, a preliminary design was obtained using classical laminate theory and the following assumptions:

- Both the LOX tank and the propellant tank must withstand an internal pressure of 1000 psi
- The Helium tank must withstand an internal pressure of 5000 psi
- An aluminum liner of thickness 3/32 in is present on the whole inner surface of the COPV
- Insulation of thickness 0.6 in and density of 115 kg/m3 is present around the COPV
- The composite shell takes all of the loading from the pressure

Using those assumptions, the loading present on the composite shell can be computed using the following equations:

$$N_1 = \frac{pD_C}{4}$$

$$N_2 = \frac{pD_C}{2}$$

Where p represents the internal pressure in the COPV and D represents the inner diameter of the COPV. Figure 7 shows a schematic of the COPV design parameters, as well as the cross-section of the tanks.

For each tank, a layup was generated using the team's Matlab script. Those layups feature the optimal angle of the plies in order to obtain the thinnest and lightest COPV possible. Since commercial COPVs are usually manufactured using filament winding, it is highly likely that is will be possible to position the plies accurately according to the optimal angles. The results of the layups were compiled in Table 3.It is important to note that uniaxial plies are used and not a weave material, meaning that each layer is either +theta or -theta. There are then an equal amount of +theta plies than -theta, since the number of layers for each layup is even.
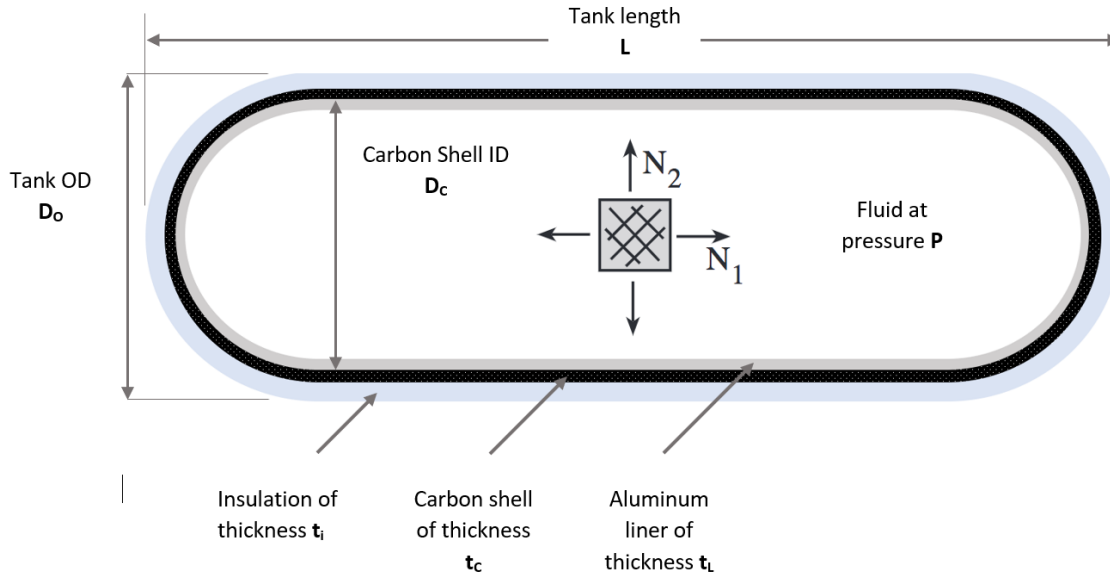
Figure 7   Diagram of COPV cross-section and design parameters

AS4/PEEK thermoplastic carbon fiber material was selected for the design of all three COPVs, due to its optimized properties for this specific application. For comparison purposes, a layup was generated for the Helium tank using T300/N5208 Carbon Fiber material, which has the same layer thickness and density as the AS4/PEEK material. To obtain a safety factor of 1.5536, a total of 192 layers is necessary, making the thickness of the composite shell 2.4 cm thick. Using AS4/PEEK then results in a much lighter tank than with other carbon fiber materials. The drawback of this selection is that AS4/PEEK is much more expensive to purchase and manufacture.

As one of these tanks will be containing liquid oxygen, testing will be done in accordance with ASTM D2512-17: Standard Test Method for Compatibility of Materials with Liquid Oxygen.

	LOx Tank	Fuel Tank	Helium Tank
Material	AS4/PEEK	AS4/PEEK	AS4/PEEK
D_o (in)	14	12	14
D_c (in)	12.56	10.64	13.05
P (psi)	1000	1000	1000
L (in)	90.69	70.28	31.38
N1 Loading (kN/m)	550.0	465.8	285.7
N2 Loading (kN/m)	1100.1	931.7	571.4
Carbon thickness (mm)	3	2	12
Number of plies	24	16	96
Layup Angle (deg)	53	53	51
Safety Factor	2.40	1.89	1.75
Failure Criterion	Hashin	Hashin	Hashin
Mode of Failure	Matrix Tension	Matrix Tension	Matrix Tension

Table 3   COPV Design Results

4. Tank Characterisation

Propellant flow to the combustion chamber will be pressure-fed. Pressure will be provided by a COPV full of helium.

$$V_{He} = \frac{P_2 V_{tanks} T_1}{P_1 T_2 - P_2 T_1}$$

$$m_{He} = \frac{P_2 \mathcal{M}_{He}}{R T_2} V_{He}$$

Ideal-gas calculations (helium remains approximately ideal below 6000psi; subscript 1 refers to compressed Helium, subscript 2 to expanded) indicate that in order to maintain a propellant tank pressure of 1000 psi throughout combustion, it is necessary to keep a 5000 psi helium tank aft of the two propellant tanks.

In order to determine the thickness of tank walls necessary to sustain a given pressure, we take

$$t = \frac{PD}{2(0.8\sigma_y - 0.6P)}$$

With the 0.8 a correction factor for geometry, $0.6P$ for wall thickness. Capacity requirements and an assumed yield strength of $\sigma_Y = 200\ ksi$ for carbon fibre thus characterise the requirements for our tanks.

5. Propellant Valves and Delivery

Two main fluid delivery systems are required for the operation of the rocket: a pressurant delivery system, and a propellant delivery system. Because the internal structure of the rocket has not yet been finalized, the following is only a functional description of these systems. The specific pipe layout will be determined once internal structure is set, with the aim of guaranteeing fail-safe operation with redundant safety features and minimized pressure drop across fluid lines.

For the pressurant delivery system, a remotely controlled regulator will be used to ensure a constant-pressure stream of helium is delivered to the two propellant tanks, keeping the propellant flow at a stable design pressure. The remote actuation of the regulator allows propellants to be loaded at lower pressures on pad while personnel is more likely to be nearby, but also ensures that ground control can control whether the rocket is ready to run or not: de-pressurized propellant tanks would not be able to generate meaningful mass flows to the combustion chamber, notwithstanding other safety features included in the propellant delivery system. The pressurant line would run down from the regulator, split, then each branch would connect to the top of a propellant tank. The required volumetric flowrate is of 0.003273 m^3 (in standard m^3 at a reference temperature of 15°C).

Next, the propellant delivery system would leverage the supplied helium pressure to deliver the propellants to the injector through simple lines. Each propellant tank would be equipped with a fail-open vent that would only be closed on launch, and a pressure relief valve for added safety. To control outflow, each tank would have a remotely actuated valve: most likely an adapted ball valve or custom design poppet valve. The valve and tubing sizing would be adapted to each propellant's mass flow: 2.6kg/s for liquid oxygen, and 1kg/s for propane. A plumbing diagram is shown in 8.

Pressure transducers are located in every tank and at the outlet of the helium tank regulator. Having two transducers at the bottom and the top of the tank allows for differential pressure measurements and therefore to estimate the liquid level in the tank, as well as providing a level of redundancy. The run valves leading to the engine are fail-closed while the actuated vents are fail-open to prevent overpressurization in the event of a failure, in addition to spring-loaded emergency relief valves. Check valves on the fill lines prevent backflow and prevent gases from escaping from the rocket via the fill lines. Each tank also has a manually opened dump valve that can be accessed in the event that the launch is aborted and the propellants need to be ejected from the rocket.
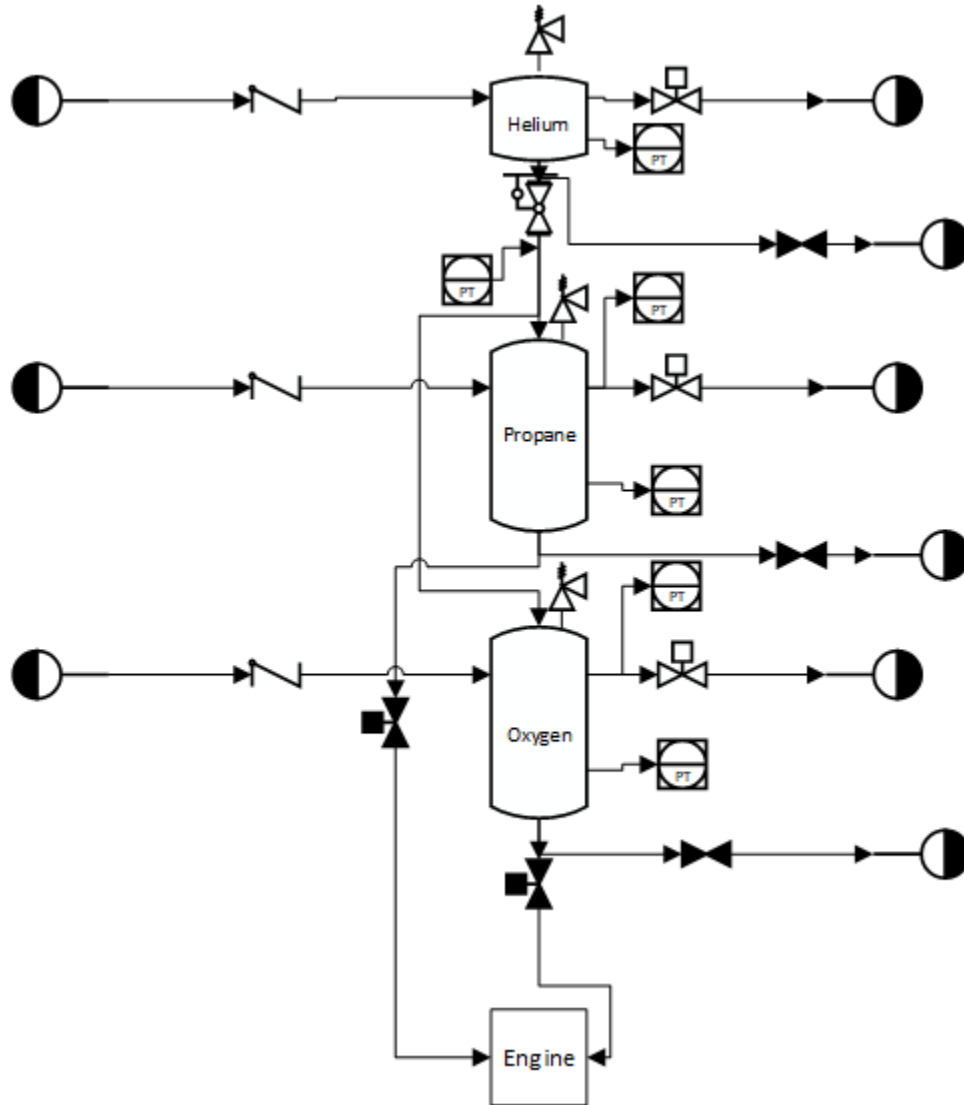
Figure 8   Inner plumbing for Ariel

6. Injector

For the injector, the team has decided to go with a pintle injector due to the combustion stability, low cost, safety and reliability. The pintle will also provide the dimensions for the combustion chamber and will receive its diameter from the external surface of the rocket. The exterior diameter of the pintle is set for now at 5.5 inches to fit with the chosen dimensions and allow for a perfect fit to the rocket wall using radial bolts. Afterwards, the length of the pintle must be decided. Following multiple runs of CFD, the length of the pintle was reduced to around 96 mm to reduce weight, space used and dead zones in the combustion chamber.

Next, the outer parts of the pintle needs to be designed. The central part, the pintle, will have a diameter of 0.04 m and will carry the Propane on its side to the exit. The sleeve (surrounding the pintle) will be used to carry the Oxidizer up to the exit. The inner part of the sleeve will constrain the flow to a specific exit area and will distribute the flow using chevrons. The pintle has one entrance area at the top with a diameter of an 1/8" to allow for a tube to carry the propane in. The oxidizer will have 2 entrances with a diameter of 1/4" at the top of the outer cylindrical part. The outer cylindrical part surrounds the sleeve and is used to constrain the LOX flow to a specific exit area. The pintle will expel the fluid outwards from 4 holes towards the inner part of the sleeve. The fuel will take the shape of a circular sheet into

18

the inner sleeve surface and the oxidizer will follow the same pattern on the external sleeve surface. The central fuel flow then hits the bottom of the pintle (a 115 degree ramp) that propels the liquid outwards where it meets with the LOX coming from the outer sleeve. Finally, the outer cylinder is separated into a top and bottom part to ease manufacturing. The top outer cylinder will connect to the bottom using six 3/8" square bolts that are 1.5" long. The only additional role of the top part is to be bolted to the walls of the rocket using radial bolts.
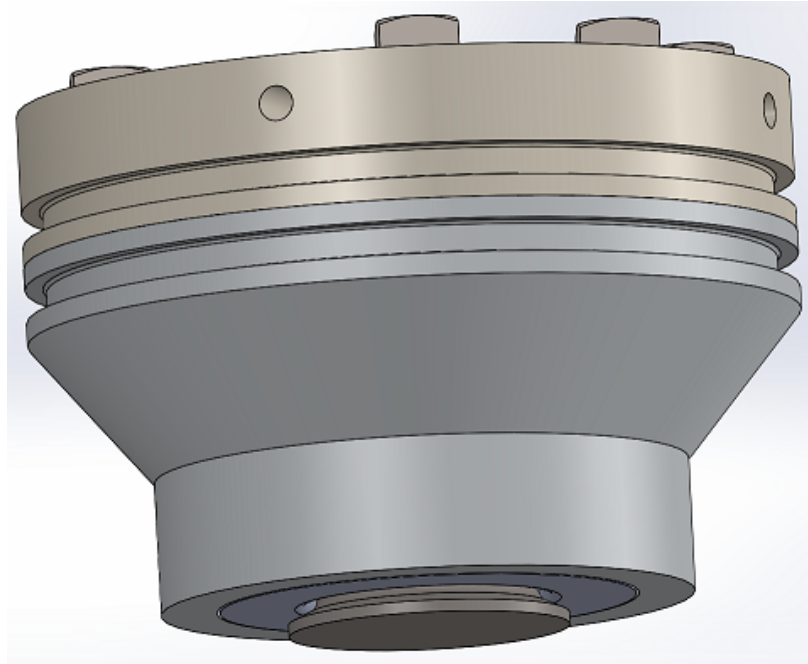

Figure 9   Current Pintle Design

The pintle was designed to provide and spray effectively 3.7 kg/s of LOX/Propane mix. This flow rate is distributed so that the propane exits at 1 kg/s and the LOX exits at 2.7 kg/s from the pintle injector. With the corresponding mass flow rates, the exit area and tunnel can be controlled to obtain the proper distribution, flow rate and angle. The following exit area were determined using CFD: 0.000603 cubic meters for the LOX exit area and 0.000589 cubic meters for the Propane exit area.

For the thread, the pintle is threaded at the top and is connected to the sleeve. The sleeve has thread on the inside and outside surface. The outside surface matches with the thread on the top outer cylinder. The injector comprises 6 O-Ring groove; two on the outside to stop the flow from the combustion chamber, two around the LOX pipes between the two parts of the outer cylinder and two on both sides of the sleeve to stop the propane and LOX from leaking out of the top. The pipes used for the inflow have NPT thread at the top to get attached to the pintle and the top outer cylinder.

Multiple runs of CFD were performed to obtain the proper flow distribution and mass flow rate at the exit. Figures 10 and 11 show the distribution and exit velocity of flow for the propane and then for the LOX.
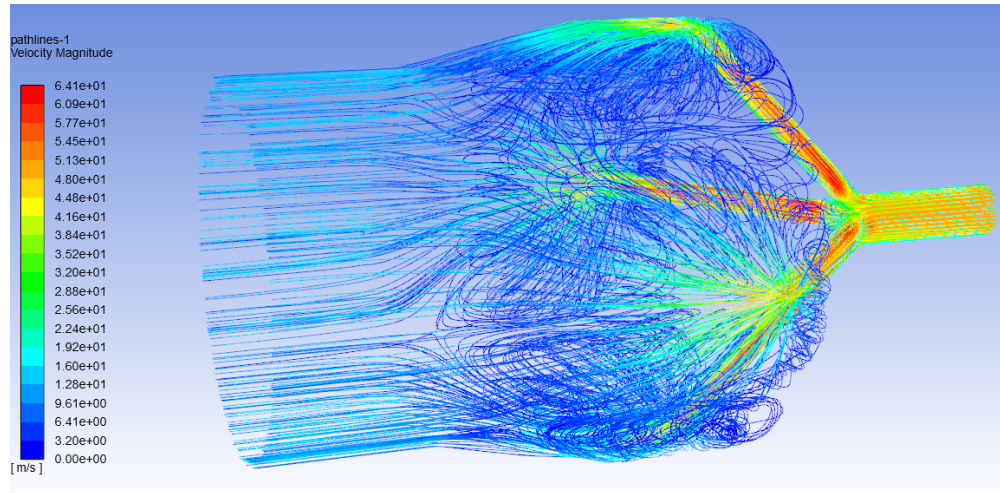
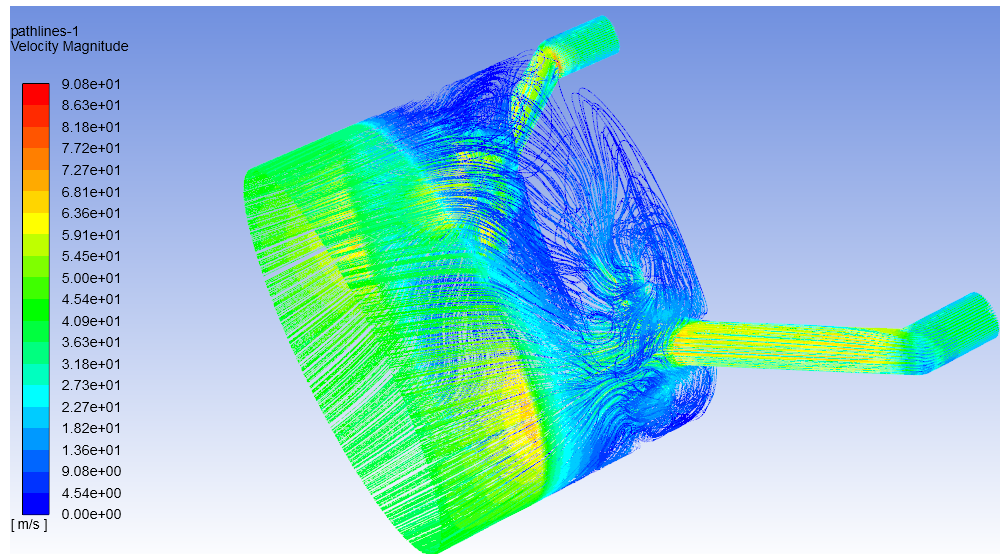**Figure 10   Internal Velocity Distribution for Propane**

Figure 11   Internal Velocity Distribution for LOX

Figures 12 and 13 show the entire pintle injector flow internally then a 2D cross-section of the flow as it enters the combustion chamber (without the combustion process):
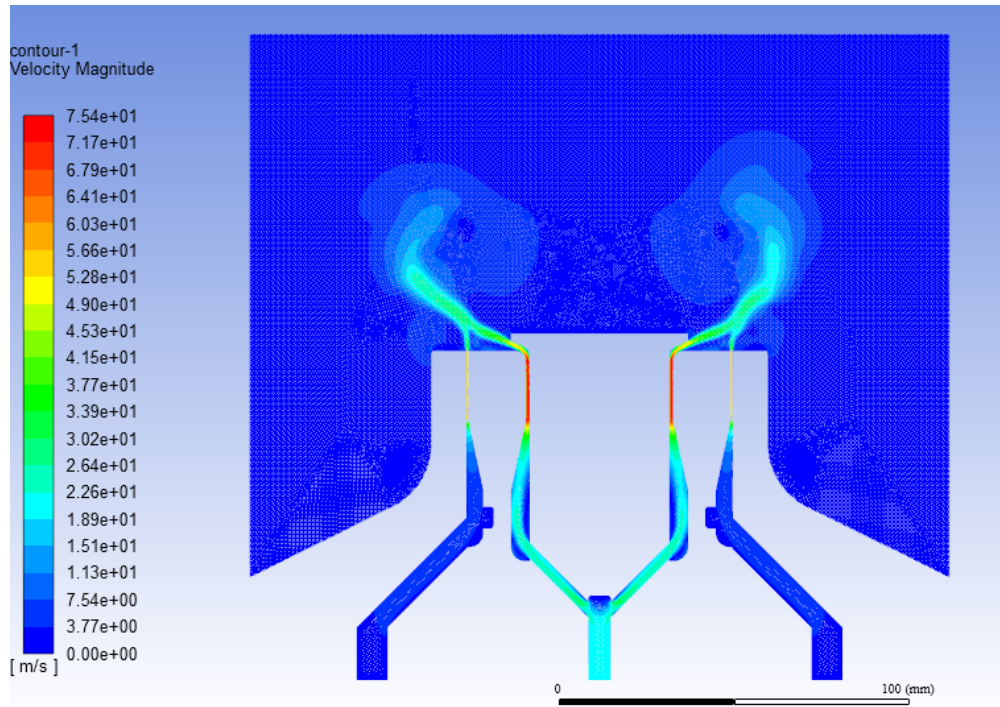
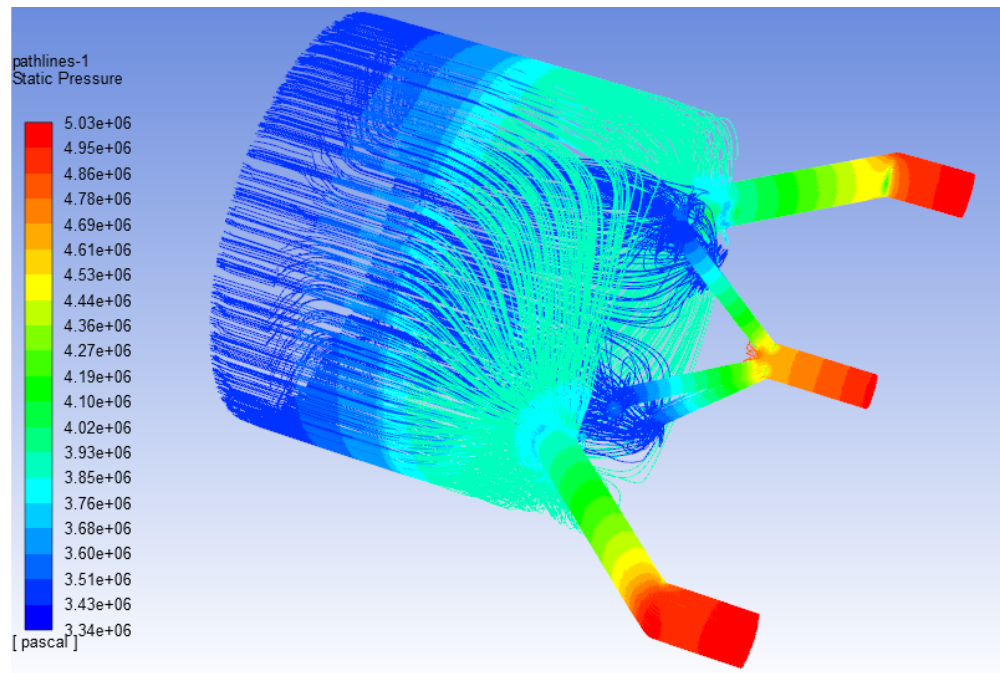**Figure 12   Injection of Propellants in the Combustion Chamber**

Figure 13   Overall Internal Flow Pressure Distribution for LOX and Propane combined

The following cross-section shows the internal system in charge of distributing the flow properly around and into the combustion chamber at an optimum velocity. Included is also an exploded view to better grasp the geometry of each part. Note that the blue-gray piece has a chevron on both sides. These are used to get an excellent LOX distribution around the cylindrical parts before entry in the combustion chamber. Propane exit velocity is around 14 m/s and LOX

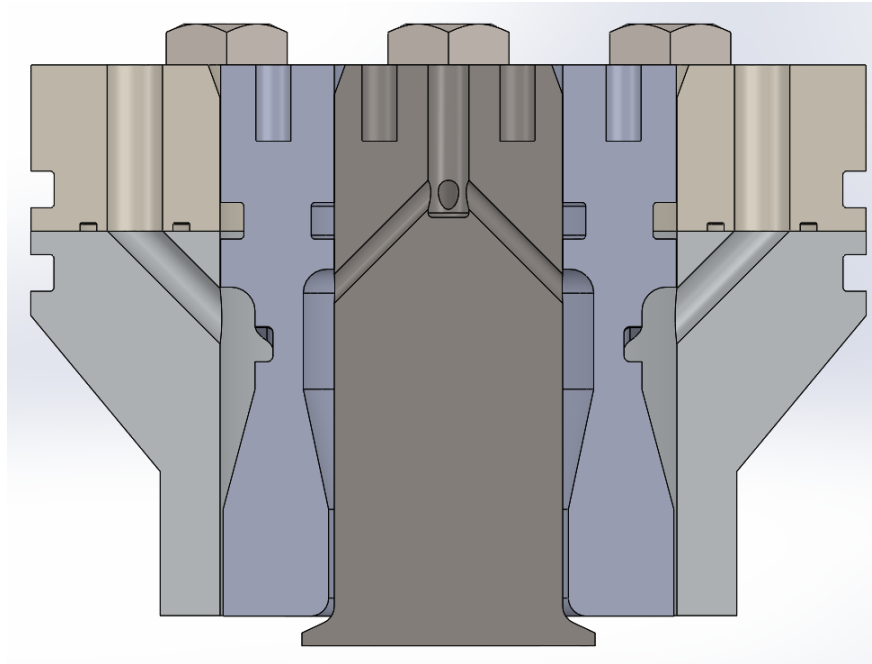exit velocity is around 40 m/s: Figures 14 and 15

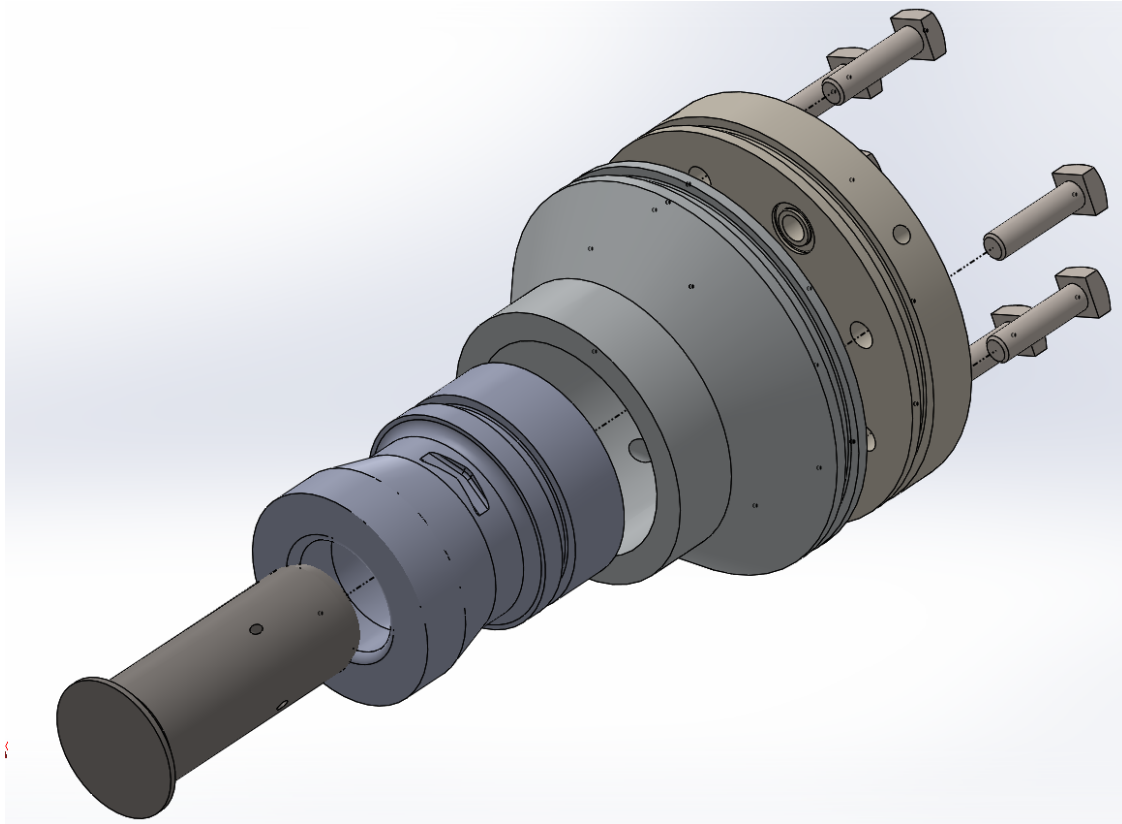**Figure 14   Overall Cross Section of the Pintle Injector**

Figure 15   Assembly of the Pintle Injector

The pintle (central part) is the part that will be most affected by the hot combustion gases from the combustion chamber since the rest of the parts are protected by the re-circulation of cold propellants on the sides of the pintle. Figure 16 shows an FEA of the temperature distribution in the aluminum Pintle after 120 seconds of exposure to a temperature of 3400K coming from the chamber while being cooled by the liquid propane flowing on its side:
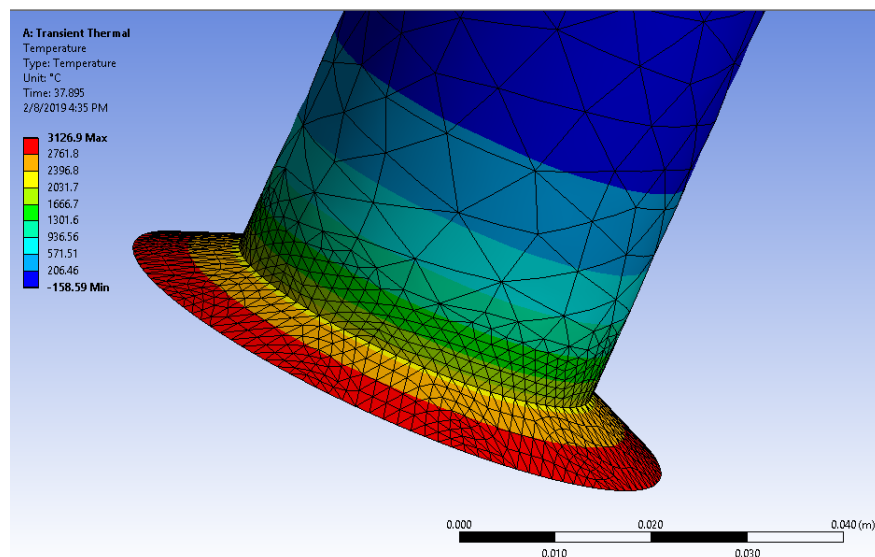

Figure 16   Aluminum Pintle Internal Temperature after Two Minutes after Launch

A stress analysis was also conducted for the entire pintle assembly to determine the weak points and the possible problems that may arise during launch. The worst deformation happens at the tip of the pintle due to the high pressure coming from the combustion chamber. Stress is not a problem in the injector. The maximum stress occurs at the extremity of the pintle next to the combustion wall. Figures 17 and 18 show these stress analysis.
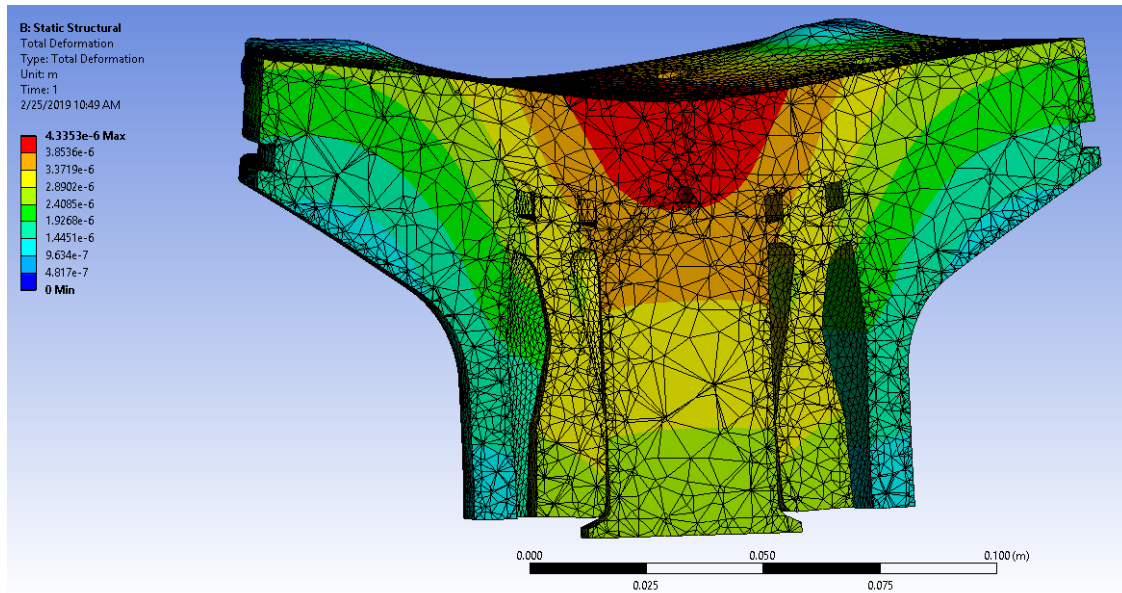
Figure 17   Deformation of the Pintle Injector with Internal and External Pressures Applied
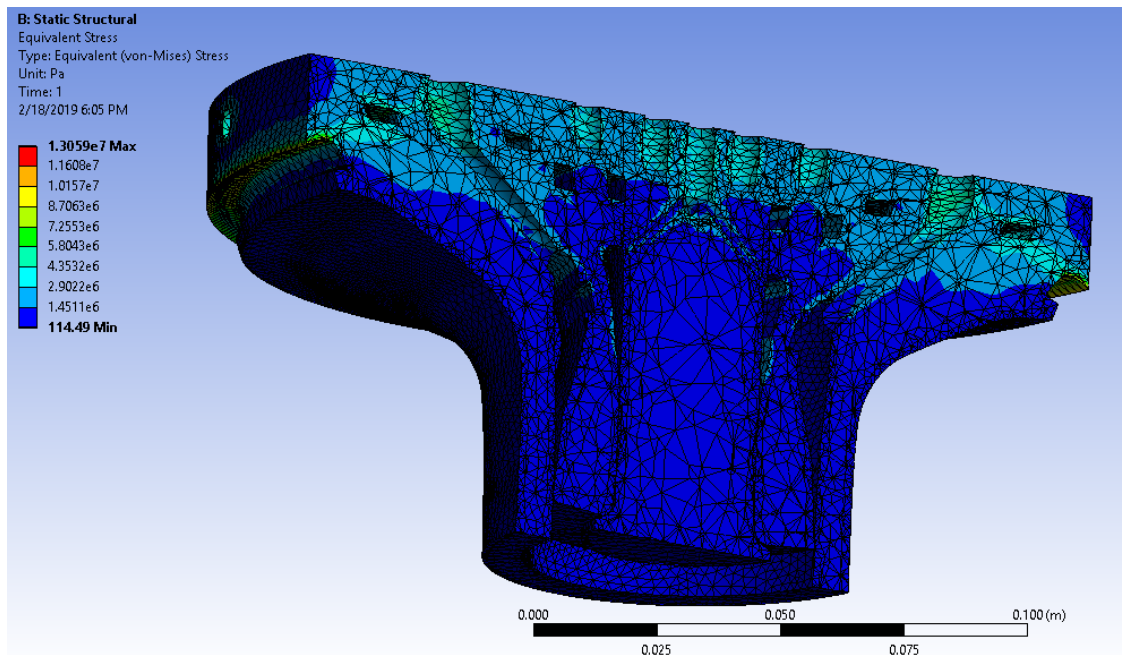
Figure 18   Stresses on the Pintle Injector with Internal and External Pressures Applied

The nominal weight for the Pintle Injector is of 2.66 kg while being completely made out of aluminum (excluding the weight of the bolts, O-Rings and radial bolts). The current design will be manufactured and used for testing using water or CO_2 to verify the performance. An advantage of the pintle injector is the fact that the pintle can be adjusted to

increase or decrease the amount of fuel injected in the combustion chamber; essentially throttling the engine. Testing will also be done with different pintle heights to take advantage of this.

7. Combustion Chamber

The combustion chamber has been designed to be 10 inches long and with an inside diameter of 5.5 inches ($L* = 2.17m$). The top part will be connected to the pintle injector via bolts. The external surface of the chamber will be cooled via cooled propellant passing by tubes squared all around the chamber.The combustion chamber and the nozzle will be 3D printed out of Inconel 625 since it has high strength and high thermal resistance properties. The following image shows the loss in pressure from the liquid passing around the combustion chamber. This is depicted in Figure 19.
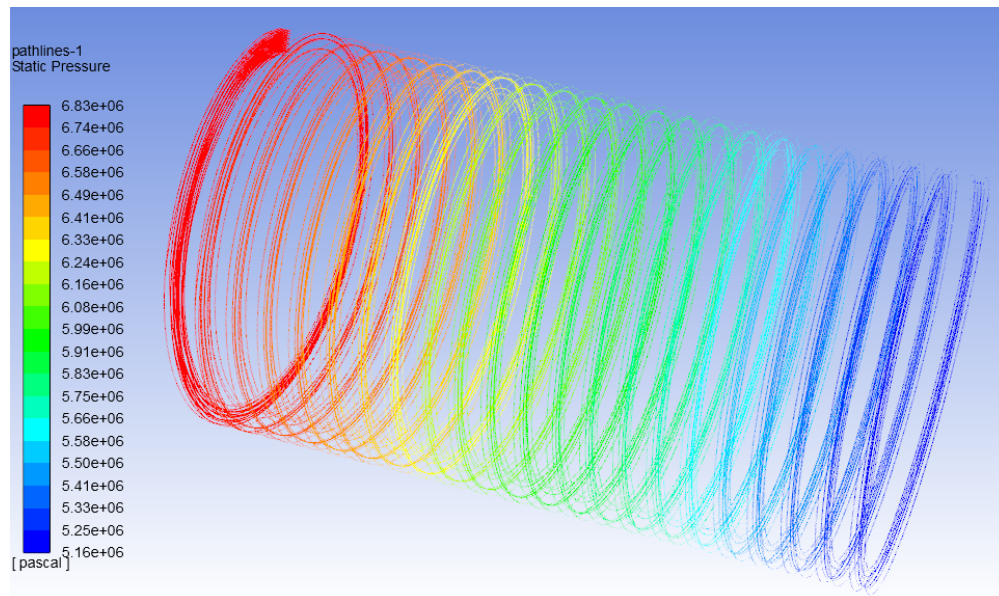
Figure 19   Pressure drop in the Combustion Chamber Cooling Pipes

The nozzle has the following dimensions: Rnozzle = 0.94", Rexit = 2.473". The dimensions were obtained using the method perviously described. The Nozzle is optimized to produce an exit pressure equal to the atmospheric pressure at an altitude of 5000 m. Figure 20 shows the combustion chamber with the cooling pipes connected to the combustion chamber.[2]
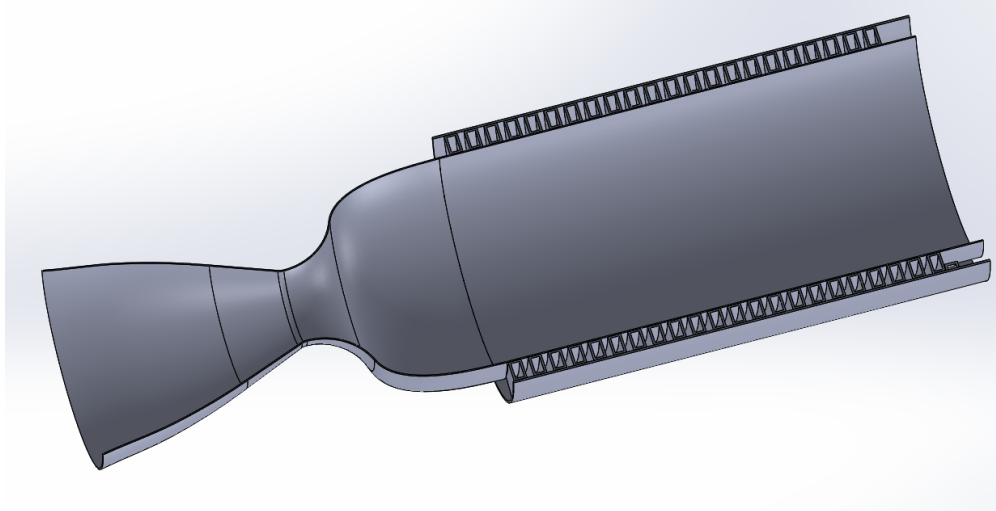
Figure 20   Combustion Chamber and Nozzle CAD Cross-Section

G. Engine Test Stand Design and Test Plan

One of the key considerations of a developing a spaceshot liquid engine is constructing an adequately equipped test facility. As such, much of the team's efforts have been focused on developing such a test site. We are in the process of negotiating a space on a rural McGill campus to build our testing facility.

Figure 21   Current Test Site Location

The space is remote and far from any human activity. About 300 feet from this location is a concrete storage building which will be used as a bunker during tests. We will purchase a shipping container and install it on the concrete pad,

bolting it to the ground and lining it with sandbags. Inside, we will install the test stand as well as the propellant plumbing. These systems will be explained in more detail in the following sections. The main features of the test site are:

- Bipropellant storage and pressurization
- Cryogenic handling capability
- 1500 psi operating pressure
- Purge capability
- Real-time pressure, temperature and video monitoring
- Remote valve actuation and venting capability

1. Test Stand

Our current test stand design is based off of a repurposed stand that will be upgraded to be able to accommodate the *Prospero* engine. The current hot-fire rocket test-stand of the McGill Rocket Team (shown in Figure 22) can withstand 6.67KN of thrust with safety factor of 2. However, for the Base 11 challenge, the rocket is estimated to have a thrust of 11KN. Therefore, the propulsion sub-team has to redesign the test-stand to withstand 11KN of thrust with safety factor of 2.
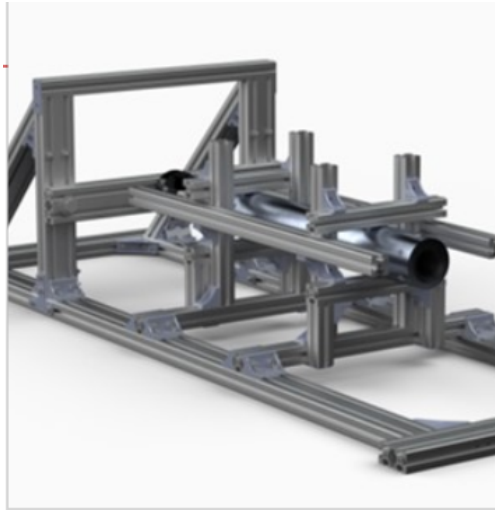
Figure 22   Current rocket test stand

During the redesigning process, two major designs for the new test-stand were made before arriving at the final design. The first modification of the new test-stand (shown in Figure 23) consists of adding three 40x80 aluminum extrusions at 45-degree angle on the middle cross-bar. The angle of 45 degree is chosen, because it was found in the free-body diagram on the added extrusions that this is the most efficient way of distributing the thrust experienced on the cross-bar. This design was rejected due to an inefficient used of material and spacing complications. The second design is very similar to the final design. It consists of adding only two 40x80 aluminum extrusions at 45 degree on the middle cross-bar and attached to a base plate of 40x120 aluminum extrusion on the ground. This design is rejected as it fails to support the thrust at a safety factor of 2. Therefore, in the final design of the new test-stand (shown in Figure 24), the two 40x80 extrusions were replaced by two 40x120 (HFS) aluminum extrusions to strengthen the structure. The base plate is replaced by a 40x160 extrusion to facilitate the attachment.
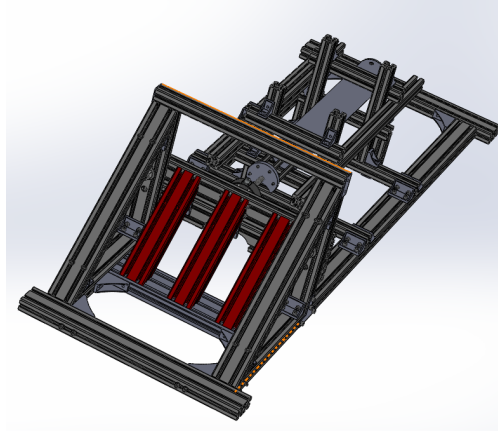
Figure 23   Main modification to test stand
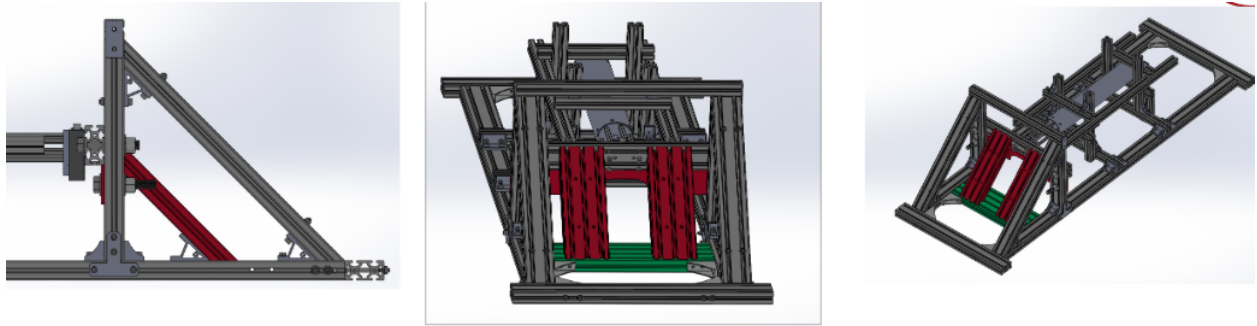
Figure 24   Current state of rocket stand redesign

To get a rough estimate of the shear stress on the new test-stand, free body diagrams were drawn and analyzed on the added aluminum extrusions (approximated as hollow rectangles) and on the middle cross-bar. To ensure the safety of the structure, Finite Element Analysis in SolidWorks were run on the part of the test-stand that supports the most thrust. The studies focused on the stress and the displacement analysis of the test-stand under 11KN and 22KN of thrust separately. The maximum stress (at 11KN of thrust) on the test-stand is 15 800 psi and occurs on the added extrusions near the middle cross bar and the base plate. Since the yield stress of the aluminum (6061 alloy) is 40 320 psi, the yield margin of safety is 27.6% at safety factor of 2. This means that the system has a safety margin of more than 2. The maximum deformation at 22KN is 2.145 mm. This is within the acceptable range of strain because the elongation at break of the 6061-aluminum alloy is between 4.8 – 10 mm. The FEA studies on 22KN of thrust are shown in Figure 25.
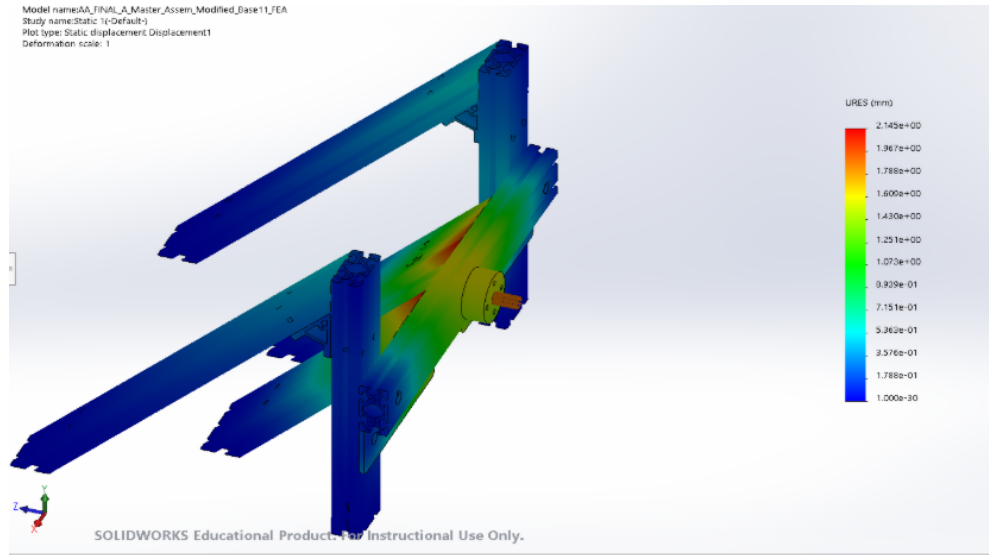
Figure 25   FEA analysis of thrust load on stand

A few issues with the design were pointed out by engineers from the Canadian Space Agency. The main issues are: 1) risk of loosening on bolt attachments and connecting hardware due to vibration of the test-stand, 2) risk of shearing stress and bearing stress failure on the base plate 3) risk of failure of part of the system due to vibration and natural frequency.

The current challenges for this project avail to be running precise FEA studies on bolts of the base plate and studying the effects of vibrations on the test-stand. Therefore, the next step of this project will be to run FEA on the shear stress and the bearing stress of bolts with ANSYS software (since the SolidWorks software is not ideal for small and precise studies). The effects of vibrations of the test-stand system will also be measured using strain gauges and studied. In addition, if the results of the FEA studies on the bolts and the connecting hardware indicate that they fail to meet the requirement, the alternative of welding may be considered to replace the bolts and hardware connections.

2. Plumbing

The test stand plumbing is designed to be sufficiently robust to accommodate cryogenic liquid oxygen and a cryogenic fuel at high pressures, following guidelines from the ASTM handbook on the safe use of oxygen and oxygen systems [3]. A P&ID of the system is shown in Figure 26.
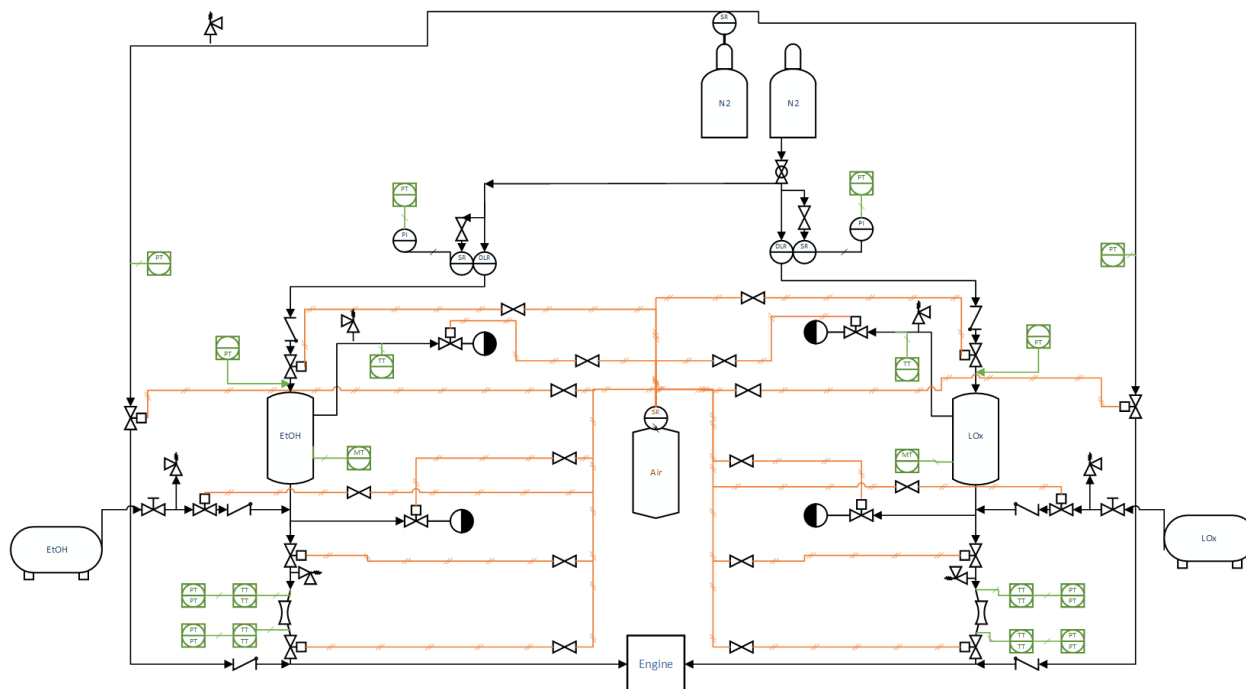
Figure 26   P&ID of test stand

The design flow rate of oxygen and propane is 5 kg/s, significantly higher than the predicted engine flowrate, in order to accommodate potential engine redesigns which would increase the required flowrate. The propellants will be pressurized with nitrogen. Two separate nitrogen tanks will be used for the oxidizer and fuel, to allow for tests to be performed at different pressures. The flowrates will be regulated with cavitating venturis for both propellants, such that the flowrates are only functions of upstream pressure. To maintain the pressure at this flowrate, a high-flow dome-loaded regulator will be used to minimize droop. The required nitrogen flowrate at 5 kg/s of oxygen is 328 SCFM, which at ambient temperature and a supply pressure of 2200 psi requires a flow coefficient of $C_v = 0.302$. The propellant valves running to the engine block are sized at 1.5" diameter to keep the flow velocity under 20 ft/s. The nitrogen tubing has a diameter of 0.5".
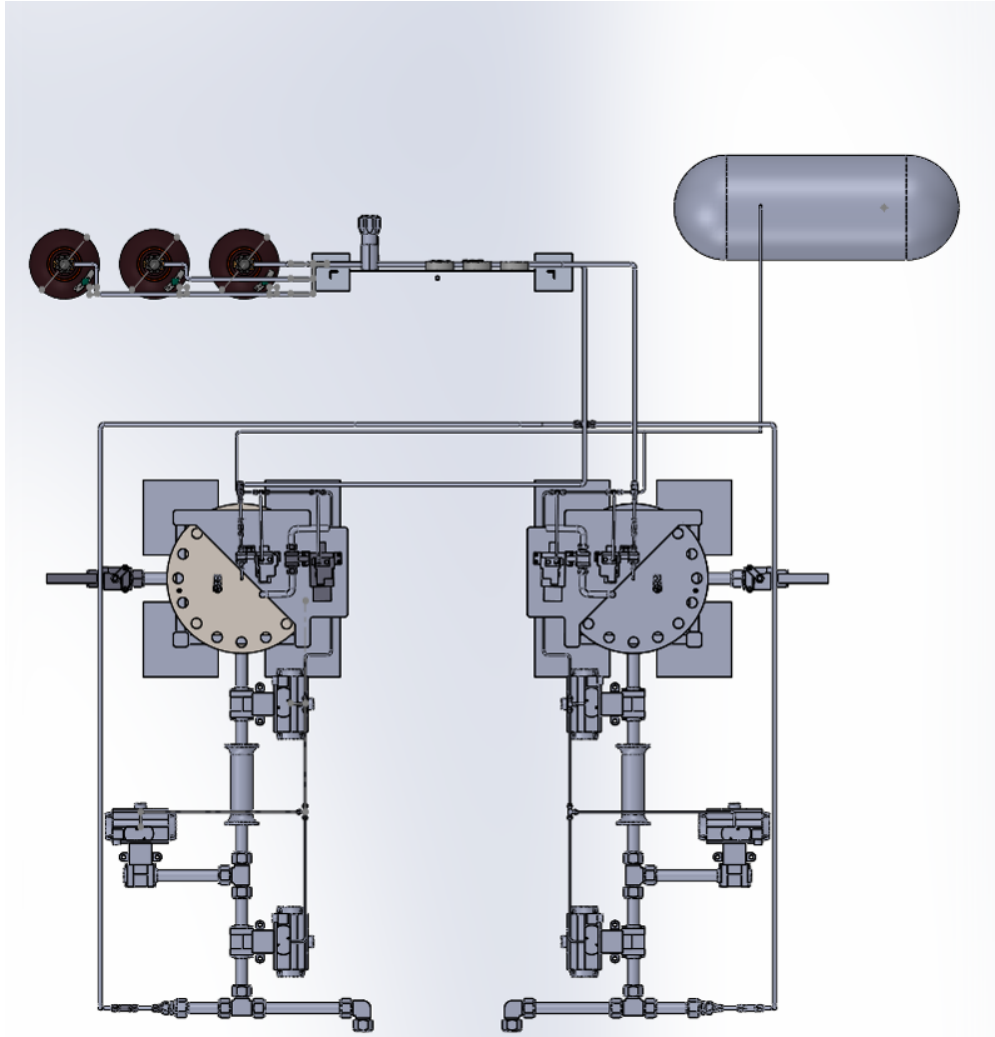
Figure 27   Overhead view of CAD of test plumbing

The test stand plumbing will be constructed from 316 stainless steel, which is both sufficiently strong to withstand the operating pressure and relatively unreactive with LOx. Double ferrule compression fittings are used throughout the system wherever possible. AN and NPT threads are also used as necessary. NPT fittings on the liquid oxygen side will be avoided, as the plumber's tape tape used in NPT threads could contaminate the system. All cryogenic ball valves are stainless steel 304 with Kel-F seats and are unidirectional with drilled balls to prevent overpressurization from trapped cryogenics. Relief vents are strategically placed throughout the system at "dead volume" regions where fluid can become trapped. Relief valves, in all cases, are all sized for the worst case scenario. All of the actuated valves fail closed, with the exception of the run tank vent valve, which fails open. Two ball valves are used between the run tanks and the engine block, adding a redundancy in the event that one valve becomes damaged or is otherwise unable to close.

Figure 28 Full assembly of test site, with plumbing, test stand and shipping container

The vent assembly features one actuated fail-open ball valve and a pressure relief valve. The worst-case flowrate will either occur during filling, when the tank is chilled by incoming liquid oxygen, or if the nitrogen regulator is stuck open at the maximum flowrate of 840 SCFM with a regulator flow coefficient of $C_v = 0.8$.

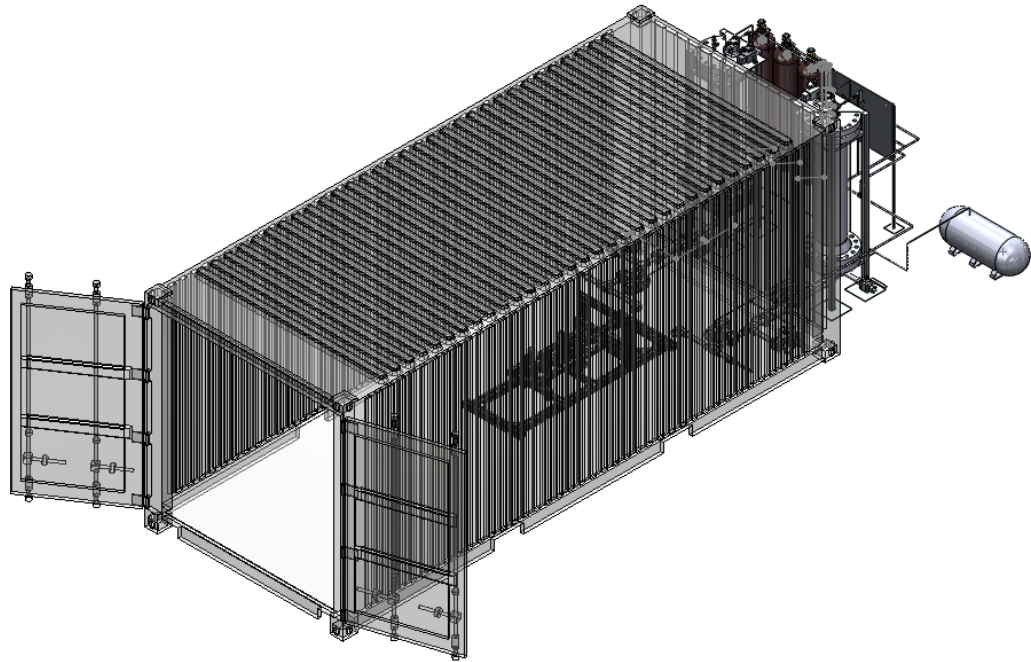The ball valves are all pneumatically actuated with compressed air, with the exception of the fill valves which are hand-actuated. Controlling the pneumatic lines are solenoid valves connected to a control board and operated at a distance. The air supply tubing is 0.25", and the solenoid valves are all fail-close and explosion-proof.

The pressure vessels are designed based on the ASME Boiler and Pressure Vessel Code guidelines and will be built from stainless steel 304. They are built from a 12" schedule 40 pipe and ASME Class 600 pipe flanges. This solution is robust and will easily be able to withstand our design pressure, but is very heavy due to the thickness of the flanges, weighing in at over 900 lbs. Although not an issue for operation, having tanks this heavy will pose significant difficulties during initial construction, and as a result we are currently re-examining our design to see if an alternative shape can result in weight savings.

All the components used for the liquid oxygen must be cleaned for oxygen service in order to prevent any possible ignition due to contamination with small particles and hydrocarbons. We will be thoroughly cleaning all components in a water and BlueGold industrial cleaner bath and will be using ultrasonic cleaning for smaller parts. For drying, we have designed and are building a HEPA filtered laminar flow cabinet to prevent any recontamination of cleaned parts. Once the plumbing is clean and dry, we will be sealing them in polybags for long-term storage. This procedure will be repeated for the oxidizer plumbing for every hot fire event or whenever deemed necessary by the Chief Safety Officer.

3. Instrumentation and Control

Pressure transducers, thermocouples, and load cells will be used to measure pressure, temperature, and force characteristics of the test stand in real-time. The analog signals from these sensors will be processed and converted to digital form

using a Labjack T7 DAQ system. A desktop computer will communicate with the T7 DAQ through a 300 ft Cat 6 Ethernet cable connection. An operator will monitor the desktop computer as it displays and records incoming data in real-time.

Due to the sensitive nature of 4-20 mA and millivolt output sensors, shielded cable will be used to carry the sensor signals, to mitigate electromagnetic interference. An AC/DC converter will be used to convert incoming AC power to 12 VDC power, which will be further converted to lower or higher voltages as needed. 12 V is sufficient for the power needs of most of the pressure transducers and load cells that we will be using. An uninterruptible power supply provides surge protection and will act as a source of battery power in the event of AC generator failure.
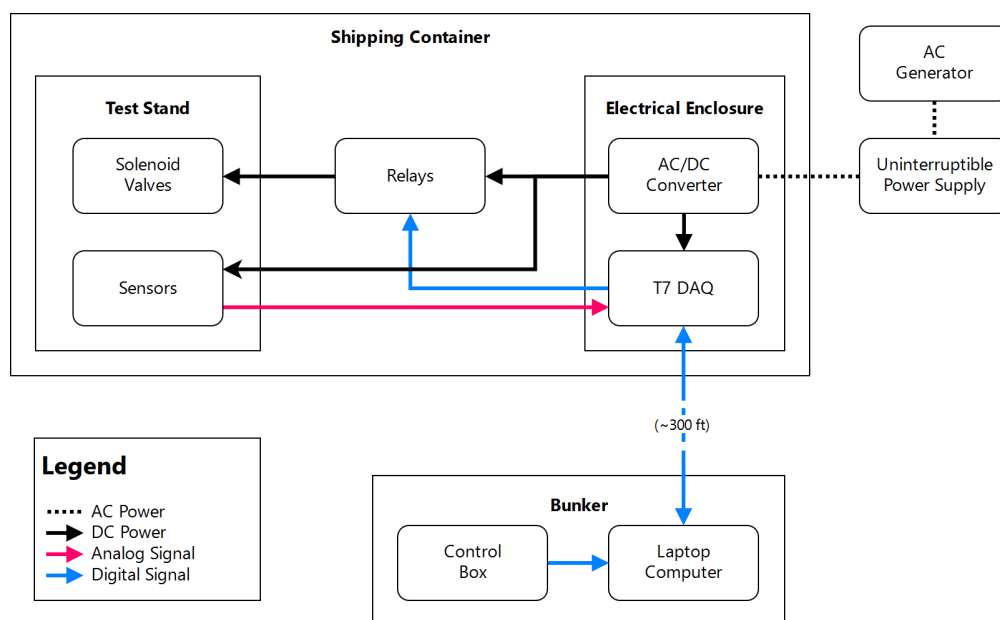
Figure 29   Overview of the instrumentation and control system

Remote control of the plumbing of the test stand will be enabled with the addition of a microcontroller. The microcontroller will be inside a control box and connected to the desktop computer via USB. It will continuously monitor switches mounted on a control board, and upon actuation of a switch, the microcontroller will send a signal to the desktop computer. The desktop computer will pass the signal to the T7 DAQ, which will actuate an appropriate electrical relay, which will actuate a solenoid valve, which will pneumatically actuate a ball valve. Figure 29 provides a basic overview of the instrumentation and control system in its live hot fire configuration. During setup and preparation the laptop computer and control box will be mobile.

4. Testing Procedures

The testing procedures are currently under development, and a complete set of procedures will only be finalized once the physical site is set up. For now, a few general guidelines have been established that will shape the development of the procedures once the picture of the test site is more complete. Safety is, of course, paramount, and to that aim the following will be done:

The procedures can be divided into three categories:

- Nominal procedures
- Contingency procedures
- Emergency procedures

Potential failure modes will be analyzed and contingency procedures will be developed to deal with every scenario. All team members will be required to attend safety training and pass safety quizzes before they will be permitted to work at

the test site.

The safest procedure is one that avoids the risk entirely. To that extent, the procedure works in tandem with the design of the test stand to eliminate exposure of personnel to hazards. All the operations and plumbing inside the shipping container are fully automated, such that no personnel will be required to enter the shipping container once the run tanks are filled. Prior to filling, the system will be purged with nitrogen gas and leak testing will be performed. Procedures will be designed to minimize the amount of necessary personnel present on the site once hazards, such as high pressure gases, are present.

5. Component Testing

Wherever feasible, individual components will be tested before integration into the full system. While the complete range of tests to every component cannot be predicted at the current stage of development, there are two major tests that will be performed before a hot fire test. All plumbing components that are to be used in the test stand will undergo hydrostatic pressure and cold shock testing prior to integration.

H. Range Safety Systems

The range safety systems remain at a premature stage of development, but the guidelines in the System Requirements document will be taken into account when the relevant subsystem is to be designed.

The primary requirements for range safety include:

- Launch abort sequence
- Remote depressurization of rocket
- SAFING and ARMING of pyrotechnic, high-pressure and fire control systems
- Isolation of engine igniter from power source with two independent inhibits
- Pressure relief devices sized for the full flow of the propellant supply systems
- Valves with appropriate failure modes to prevent unintentional opening or closing
- Pressure vessels with a minimum safety factor of 1.5

Most of the relevant safety features are discussed in detail in their corresponding sections or in the Hazard Analysis section, with the exception of the ARMING and SAFING system. For this system, we will employ arming keys, with each key specific to a different safed mechanism. The keys will create a physical disconnection of the electrical circuit providing power to the energetics, ignitor or high pressure valves. This system has previously been employed by the Team in many different launches, with great success. The following systems will be equipped with a key safing mechanism:

1) The oxygen run valve
2) The propane run valve
3) The nose cone separation mechanism
4) The pyrotechnic ignitor

4 keys will be sufficient to allow us to meet all of the requirements for SAFING and ARMING.

I. Airframe Structure

Ariel's airframe will consist of a nose cone, body tubes, couplers, fins and a boat tail. The following section will focus on the design of the body tubes of the rocket, as they are an integral part of the preliminary design of the rocket. Research, design and optimizing work is currently being done on the nose cone, the fins and the boat tail, but additional information from the engine design is needed to continue.

1. Material Selection

To progress on the design of the airframe, the material of the main components was first determined. Due to strict mass restrictions explained in section E of the present report, a decision was made to prioritize the use of advanced composite materials for as many component of the airframe as possible. Therefore, the nose cone, the main body tube, the fins, and the boat tail will all be made out of Carbon Fiber Reinforced Polymer(CFRP). As CFRP materials tend to

be much lighter compared to metals for equal strength properties, this decision will help greatly in reducing the weight of the airframe. It is highly possible that Glass Fiber Reinforced Polymer (GFRP) components will also be needed, due to the RF transparency properties of that composite. This will be confirmed later on in the design process in conjunction with the needs of avionics.

Research has been done on the properties of carbon fiber materials subjected to high temperatures and it has been identify as a concern. However, it is currently not possible to account for those high temperatures experienced without a more detailed flight pattern and flight simulator. Our reasearch however has confirmed that high temperatures will be experienced by the airframe due to skin friction drag and re-entry conditions. In order to make sure that those variations in properties are somehow accounted for in our preliminary design estimations for the airframe, the safety factors that we aimed for are significantly higher than what would normally be required.

2. Load Cases

As the engine is still being optimized, a very simplistic load case was first established, in order to obtain preliminary airframe weight estimates that can be fed to our engine optimization code.

This preliminary load case calculation takes into consideration both axial loading and normal loading on the airframe. In those preliminary calculations, effects of wind gusts and angle of attack are ignored.

Axial Loading

The axial loading at any point on the airframe can be calculated using the following formula:

$$F_{axial}(x) = -T + D_{forward} + a_x m_{forward}$$

Where F_{axial} represents the axial force acting on the rocket body cross section, T represents the thrust applied at that cross-section, $D_{forward}$ represents the total drag force acting on the airframe from the tip of the nose cone to the point x, a_x represents the vertical acceleration of the rocket, and $m_{forward}$ represents the mass of the rocket from the tip of the nose cone to the point x.

In order to find the point of the rocket where the axial force is maximized, one must know at what point on the rocket the thrust is applied. As we currently do not have this information, due to the engine attachment points not being known, it was assumed that all the thrust is transferred into the rocket at a single point, located very close to the bottom of the rocket. Using this assumption, the axial force calculated accounts for the worst case scenario possible, since all the load caused by the thrust will be accounted for. By having it positioned near the bottom, the largest drag force and the largest inertial load is also accounted for. Figure 30 shows the distribution of the axial force along a very simplified rocket model [4].
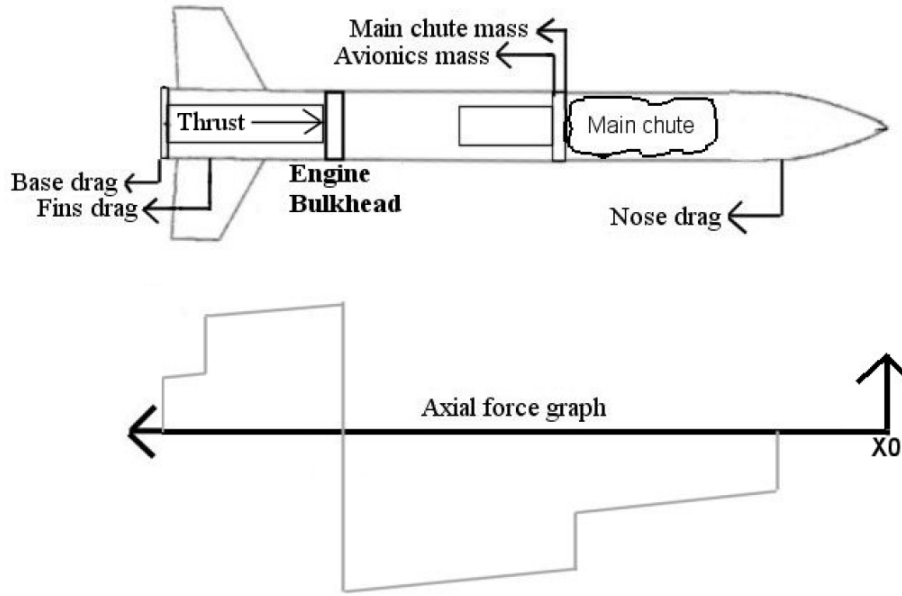
Figure 30   Axial Force Distribution Along the Length of a Rocket

Using this diagram, it is possible to write equations for the axial loads both before and and after the engine bulkhead.

$$F_{FwdOfBulkhead} = -(D_{NoseCone} + D_{Fuselage} + a_x m_{FwdOfBulkhead})$$

Where $F_{Fwd\ Of\ Bulkhead}$ represents the axial force acting on the body tube forward of the bulkhead, $D_{Nose\ Cone}$ represents the drag force applied on the nose cone, $D_{Fuselage}$ represents the drag force acting on the fuselage forward of the bulkhead, a_x represents the vertical acceleration of the rocket, and $m_{Fwd\ Of\ Bulkhead}$ represents the mass of the rocket forward of the bulkhead.

After the engine bulkhead, there is a tension load applied. As properties of CFRP materials are generally lesser under compression loading than under tension loading, the compression load forward of the bulkhead was selected as the loading to analyze.

After identifying the point along the rocket to analyze for axial loading, the critical moment of the flight must be identified. The point of maximum dynamic pressure (max Q) and the point of maximum thrust were both analyzed. A spreadsheet was generated using data from the flight simulator to calculate the worst compression load applied on the airframe during the flight. The results show that the worst compression load is experienced by the airframe 48.6s after engine ignition. The data from this point in the flgiht is summarized on Table 4. The maximum compressive load calculated on this table is the load that was used to design the airframe composites layup.

Normal Loading

From the weight budget section (section E) of this report, it can be concluded that the engine is, by far, the heaviest section of the rocket. However, the components of the engine and their attachment points has not been designed yet, meaning that both the weight distribution and the attachment points are not known. This makes it difficult to estimate the bending loads in the airframe. However, the fact that there is bending on the airframe was accounted for in the composites layup, by including more than 50% of the fibers to be +/- 45 °. This assumption should be sufficient to get decent weight estimates for the airframe without having a more refined engine design.

However, modifications will be made to the flight simulator to allow us to take into account normal loading more accurately for future design iterations. The simulator will include an option to calculate the lift generated by both the fins and the nose cone, which are two of the major normal forces acting on the nose cone. The simulator will also

36

	Max Drag	Max Thrust	Max Compression
Drag (N)	3360	844.52	828.53
Time (s)	25.831	48.481	48.6
Acceleration (m/s^2)	23.846	59.437	59.8
V (m/s)	553.03	1418.4	1427.3
Mass (kg)	284580	179381	178678
Thrust (N)	12656	13000	13012
Mach	1.81	4.72	4.74
Compressive Force (N)	10143.6	11506.4	11500

Table 4   Compressive Loading on the Airframe

include the option to add an angle of attack to the rocket, which will have a significant effect on the normal forces experienced by the rocket. Using the angle of attack, the simulator will then be able to calculate and produce a graph of the pressure force acting along the rocket in the normal direction.

Coupled to data on the mass distribution along the rocket, those modifications to the flight simulator will allow us to calculate most normal forces that are applied along the airframe during flight. Using those forces, it is then possible to draw shear-bending diagrams along the length of the rocket to identify the maximum bending moment experienced by the airframe.

3. Airframe Composite Design

In order to design the composite layup for the airframe, a Matlab program was developed using classical composite laminate theory. Using the axial load and a composite layup as the input, the software is able to compute the safety factor of the laminate using the Maximum Stress failure criteria, the Quadratic failure criteria, and the Hashin failure criteria. In the Matlab program and in this report section, the following convention was used to denote the on-axis and off-axis directions.

- On-axis direction (x,y): Defined as having the x direction aligned with the fiber direction of a ply and the y direction aligned with the matrix direction of the ply
- Off-axis direction (1,2): Defined as the loading axis of a laminate, with the 1 and 2 directions aligned with the principle loading directions

To account for compression loading on the airframe, the body tube can be modeled as a flat plate on which an off-axis loading N_1, calculated in N/m, is applied. The loading can be calculated as follows:

$$N_1 = \frac{F_{axial}}{C_{Rocket}}$$

Where N_1 represents the off-axis loading in the 1 direction, F_{axial} represents the axial compressive force acting on the body tube, and C_{Rocket} represents the average circumference of the rocket body tube cross section.

To account for bending in the body tube, a bending moment M_1, in Nm/m, can also be applied to the laminate, using the same method that was used to find N_1. However, since the geometry of the cross section affects the bending properties of the laminate, a flat plate approximation cannot be used in this case. For an isotropic material, the following moment-deflection relation is valid:

$$M_1 = EIk_1$$

However, for a composite material, this relation is not valid. The following relation must then be used as the moment-deflection relation for a composite material [5]:

$$M_1 = \int_A \sigma_1 x_3 dA$$

After a few algebraic simplifications, this relation can be simplified to the following:

$$M_1 = D_x k_1 = -D_x \frac{\partial^2 w}{\partial x_1^2}$$

The program will also be modified in order to account for buckling, humidity and temperature corrections in the future.

Using the data from Table 4, the compressive load N_1 was calculated and a composite layup was designed to accommodate that load. Complete information on the layup can be found on Table 5. This layup features more than half the plies oriented in +/- 45 °to account for bending loads for now. It is also assumed that all airframe sections will be manufactured using prepreg carbon fiber material T300/N5208.

Max compression load (kN)	-11.5
Airframe inner diameter (in)	14
N_1 (kN/m)	-10.3681
Composite Layup	[0_4/±45_4]_s
Layer thickness (mm)	0.125
Number of layers	24
Composite thickness (mm)	3.0
Core thickness (m)	0
Safety Factor	112
Failure Criterion	Quadratic
Failure Mode	Compression
Material	T300/N5208

Table 5   CFRP Layup for airframe components

An extremely high safety has been selected, due to the high level of rough estimations that have been made. A more complete loading analysis will be produced and a much lower safety factor of 5 will then be selected for the airframe. This lower, but still quite high safety factor is considered necessary, to ensure that no failure occurs during flight due to unforseen circumstances. As it is impossible to reproduce exactly the loading that the airframe will be subjected to, our team prefers to have a rather high safety factor, even if it leads to a heavier airframe.

4. CFD Work

One important component for having accurate results using our SRAD flight simulator is to have good drag coefficient data. However, our team's CFD capabilities at the beginning of the Base11 space challenge were fairly limited. We had never successfully simulated compressible flow in 3D. In order to solve that problem, the team decided to assign a nose cone optimization project to a group of senior students. Through that project, the team's CFD capabilities have increased and we are now able to simulate compressible flow. Through this project, the team was also able to get expert advice from Prof. Evgeny Timofeev of the McGill University Department of Mechanical Engineering.

Nose Cone Optimization

For this project, a group of 4 senior students were given the task of designing a nose cone that is optimised for a given flight path. As no flight path for the Base11 challenge was ready at the start of the project, they were given the flight path of the team's previous 30k COTS entry for Spaceport America Cup. Even though this flight pattern is very different from the Base11 rocket, it still reaches supersonic speed. The team was then able to make significant progress on modeling compressible flow at mach numbers up to 5 on ANSYS Fluent.

Figure 31 shows a velocity contour obtained on ANSYS Fluent at a speed of Mach 5 on a LV-Haack Nose Cone geometry.
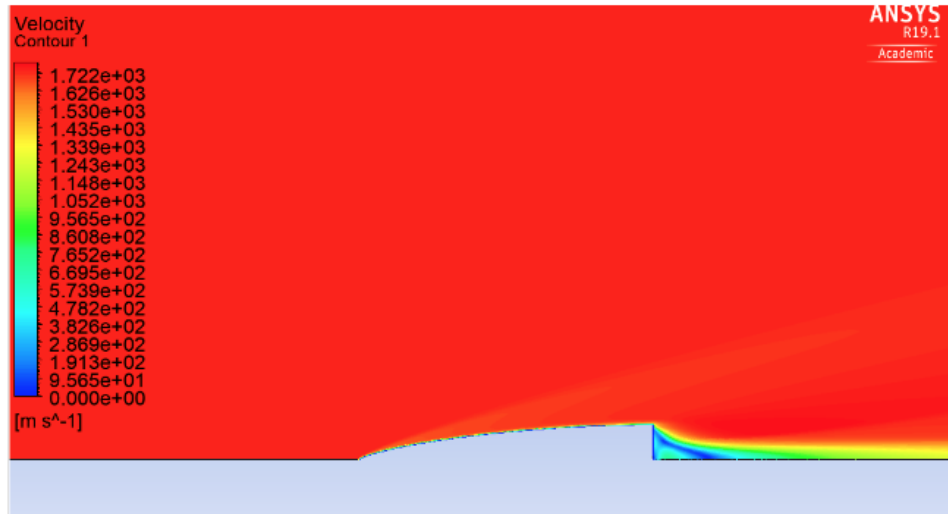
Figure 31   Velocity Contour at Mach = 5 for a LV-Haack Nose Cone

Since the team does not have access to a supersonic wind-tunnel, other methods were used in order to validate the CFD methodology. The first method that was used is comparison with analytical solutions or with literature values. A simulation was done for supersonic flow over a sphere. The standoff distance between the sphere and the shock can be found in literature, as shown in Figure 32 [6]. Figure 33 shows the values obtained by simulating this flow on ANSYS Fluent.
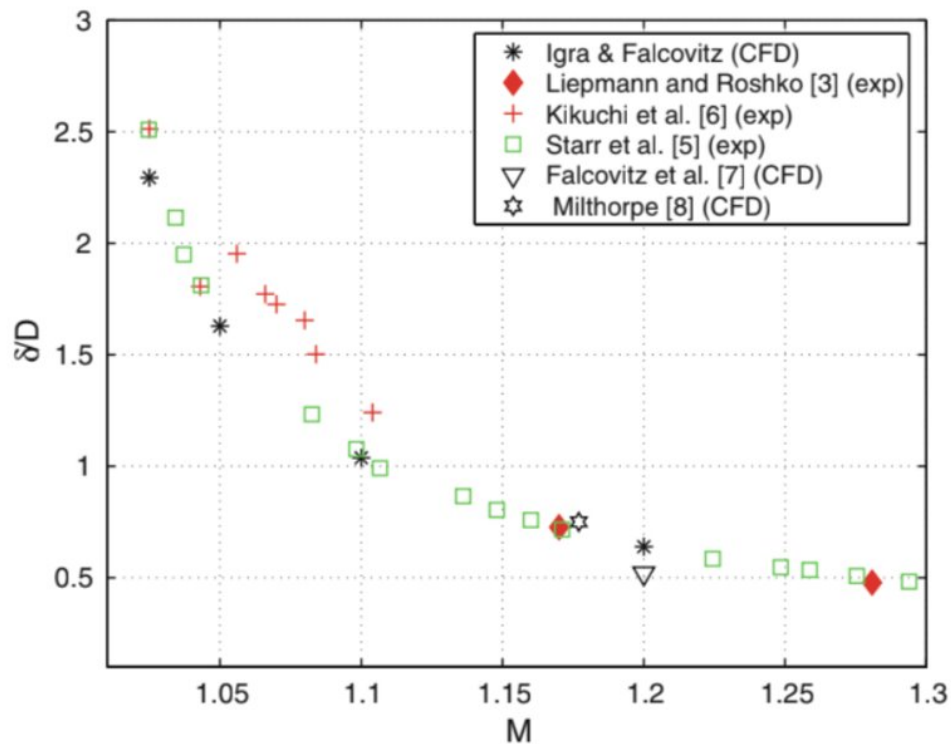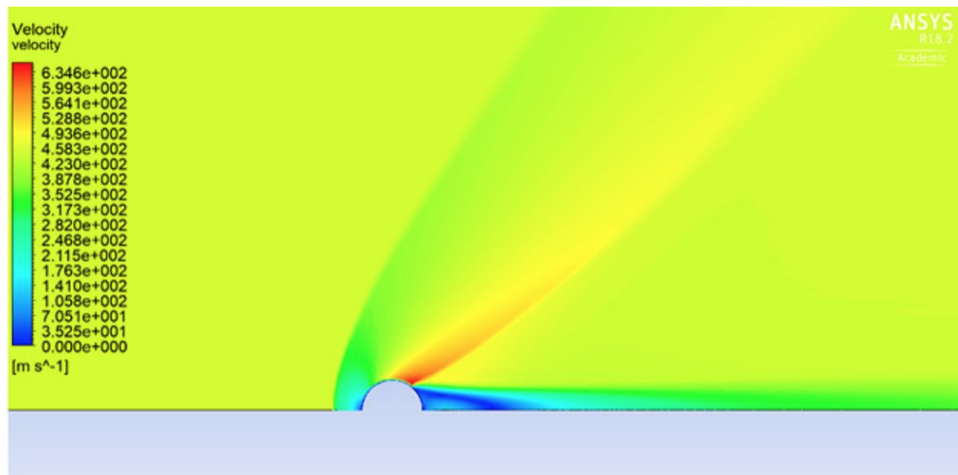

Figure 32   Literature values for shock standoff distance for supersonic flow over a sphere
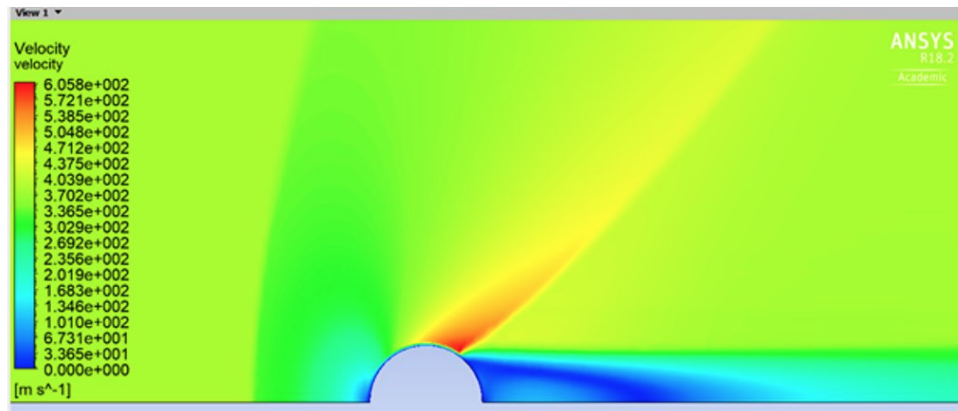
M=1.3, Δ/D=0.5

M=1.1, Δ/D=1.05

Figure 33   CFD values for shock standoff distance for supersonic flow over a sphere

Another simulation was done using the case of supersonic flow over a triangular step. For this case, it is possible to obtain the angle of the oblique shock wave with a simple equation or even from an online calculator. The model is recreated on ANSYS Fluent and the angle of the oblique shock is compared with theory to ensure that the solvers yield accurate results.

The nose cone optimization team also looked into the possibility of adding an aerospike to the nose cone of this rocket. Since this rocket will be achieving high mach numbers, it is expected to have a large pressure vessel and consequently have a large airframe. A Von Karman nose cone with a large base diameter will be long and heavy. Instead, it may be beneficial to have a short and blunt nose cone equipped with an aerospike at the tip to reduce drag and heat transfer. The nose cone will no longer have the Von Karman streamline shape, but the aerospike will help deflect the fast approaching air and reduce air particle collision with the blunt nose cone as seen in Figure 34 and 35. At hypersonic velocities, an aerospike could reduce the drag from 20 to 60 percent according to literature. Overall, an aerospike could effectively reduce drag and heat transfer while keeping a lighter and wider nose cone. The nose cone optimization team has already begun modeling, meshing and simulating different aerospike geometries. Although the final nose cone dimensions are subject to change, the team is slowly building experience and confidence in designing a nose cone adequate for the Base 11 flight pattern.
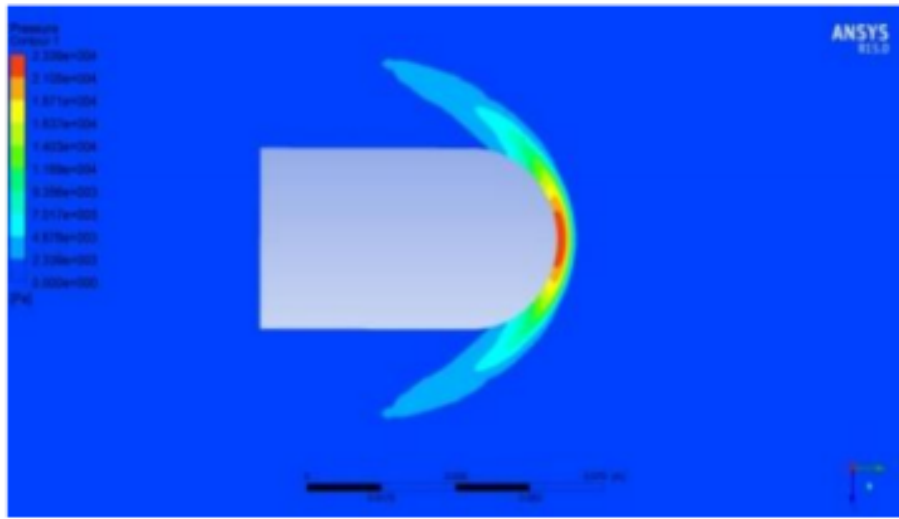
Figure 34   Pressure contours on blunt nose cone
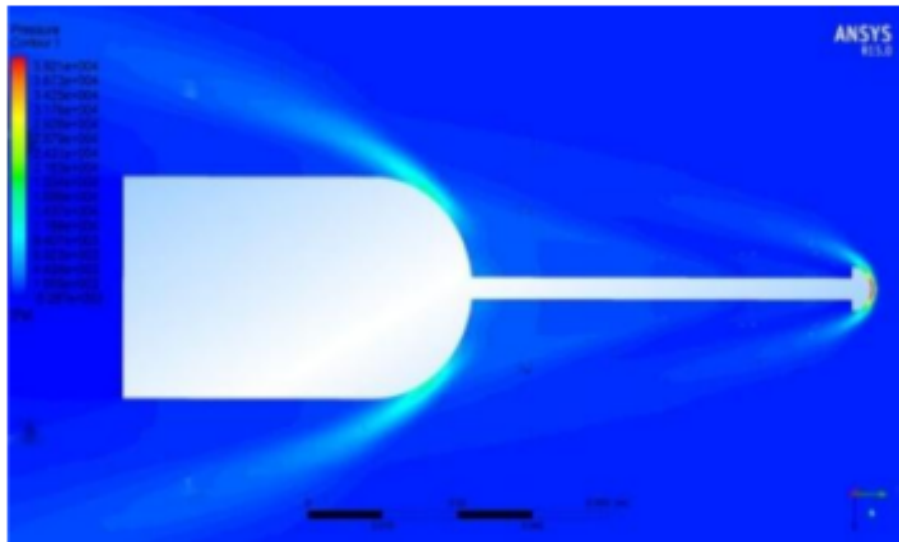
Figure 35   Pressure contours on blunt nose cone with aerospike

3D External Compressible Flow Simulations

The team has also made significant progress in simulating 3D external compressible flow to obtain drag measurements. For example, the increase in drag coefficient due to the addition of four thin patch antennas on the exterior of the rocket airframe was calculated. Figures 36 and 37 show the velocities of the simulations with inlet flow at average subsonic velocity (M=0.8) and average supersonic velocity (M=1.4) for the 30k rocket expected to fly at Spaceport America Cup 2019. To properly complete these simulations, we received help from a few graduate students who studied CFD as part of their master's degree. The size of the enclosure had to be determined mathematically to properly represent the far-field conditions. The graduate students also offered a lot of insight on the mesh sizing and inflation layers to properly model the boundary sub-layer to obtain an accurate drag coefficient value.

Velocity
Contour 1

2.796e+02
2.641e+02
2.486e+02
2.330e+02
2.175e+02
2.020e+02
1.864e+02
1.709e+02
1.554e+02
1.398e+02
1.243e+02
1.087e+02
9.321e+01
7.768e+01
6.214e+01
4.661e+01
3.107e+01
1.554e+01
0.000e+00
[m s^-1]
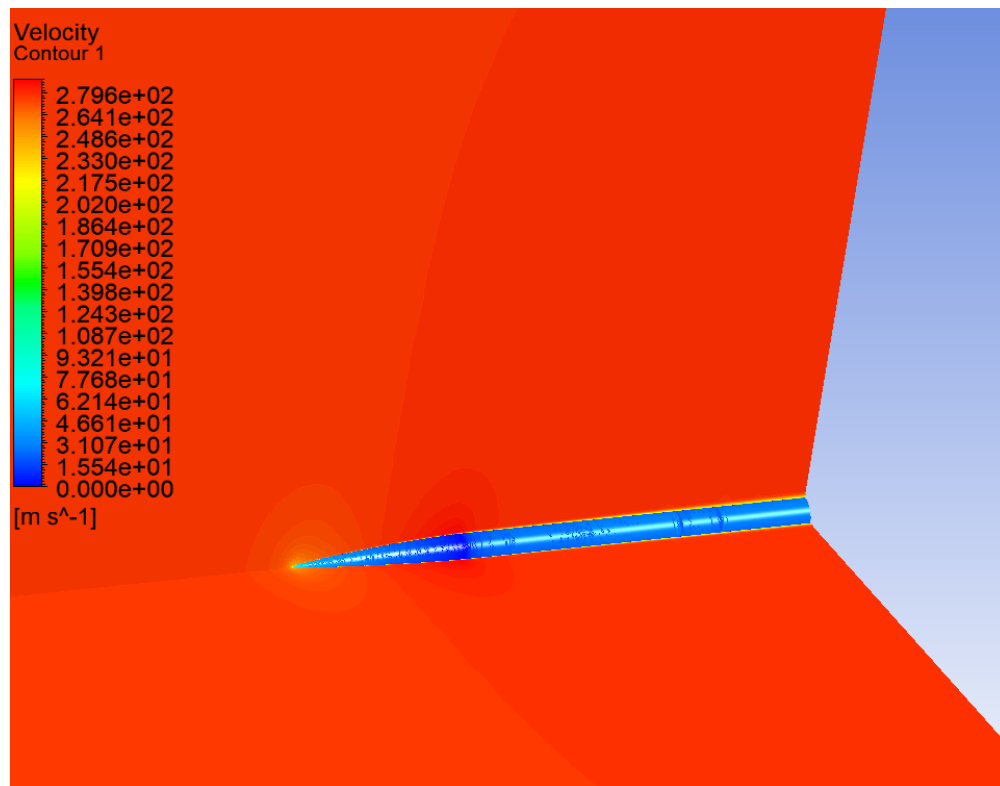
Figure 36　　Velocity contours at M=0.8
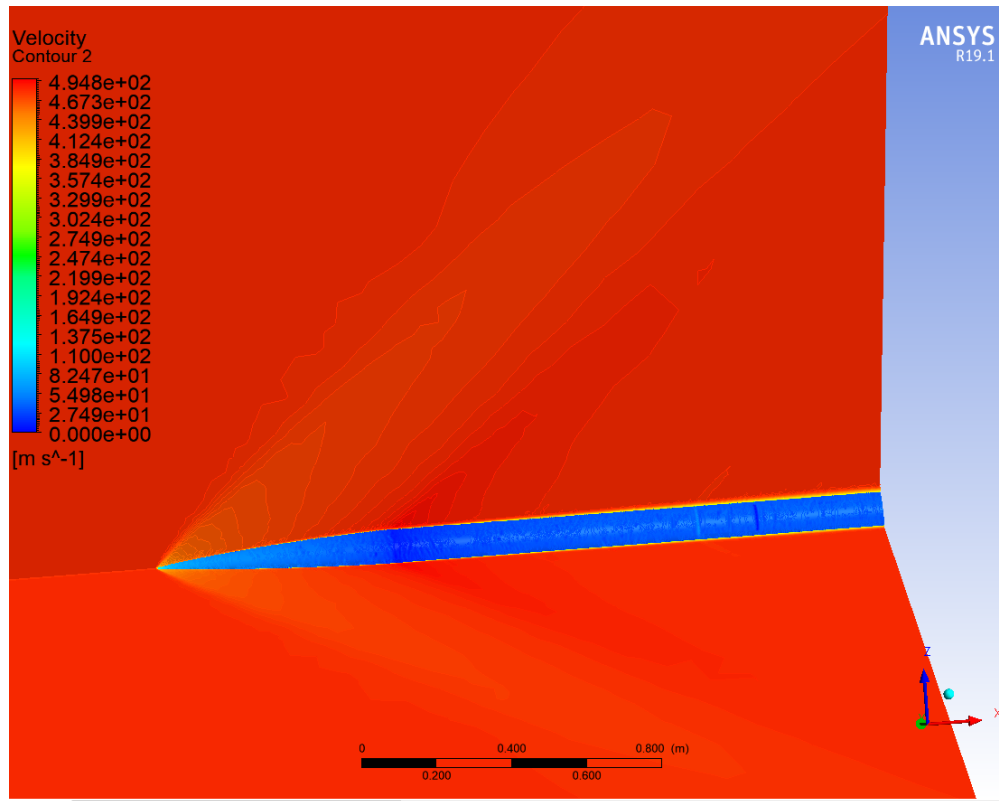
Figure 37   Velocity contours at M=1.4

We have also attempted taking into account imperfections on the rocket airframe to obtain a more realistic drag coefficient. For example, the presence of screw head protruding out of the body tube and fillets around the fins were modeled as shown in Figure 38 and 39. Those simulations were done on models of our Spaceport America Cup 30k ft COTS rocket, but a similar process will be done on the base 11 rocket. We are constantly working on refining the model by adding realistic conditions such as lateral wind, a small angle of attack, change in air density and pressure with altitude, etc. The idea is to keep reiterating our model and get a drag coefficient as close to reality as possible to use in our flight simulator and better predict the rocket's flight path.
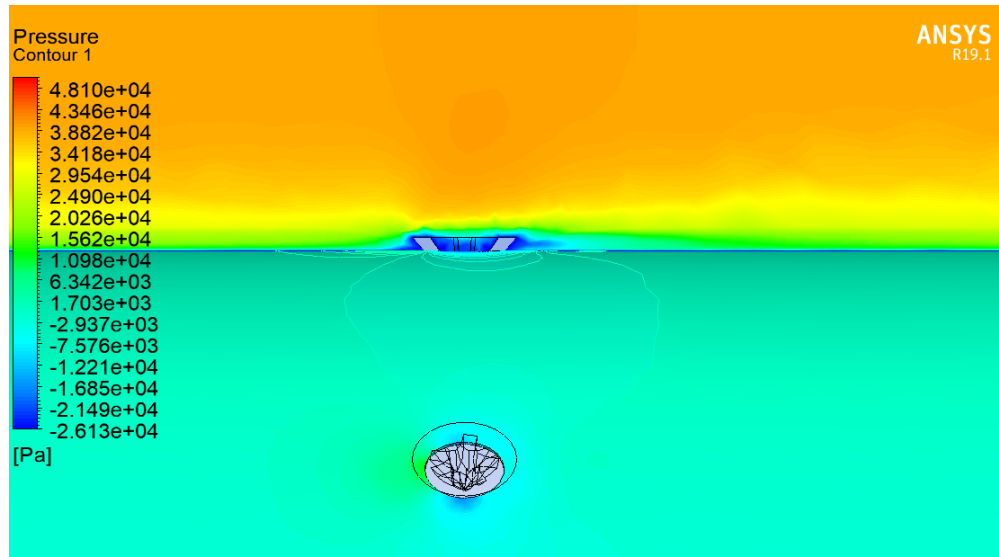
Figure 38   Flow at Mach 0.8 over the screws
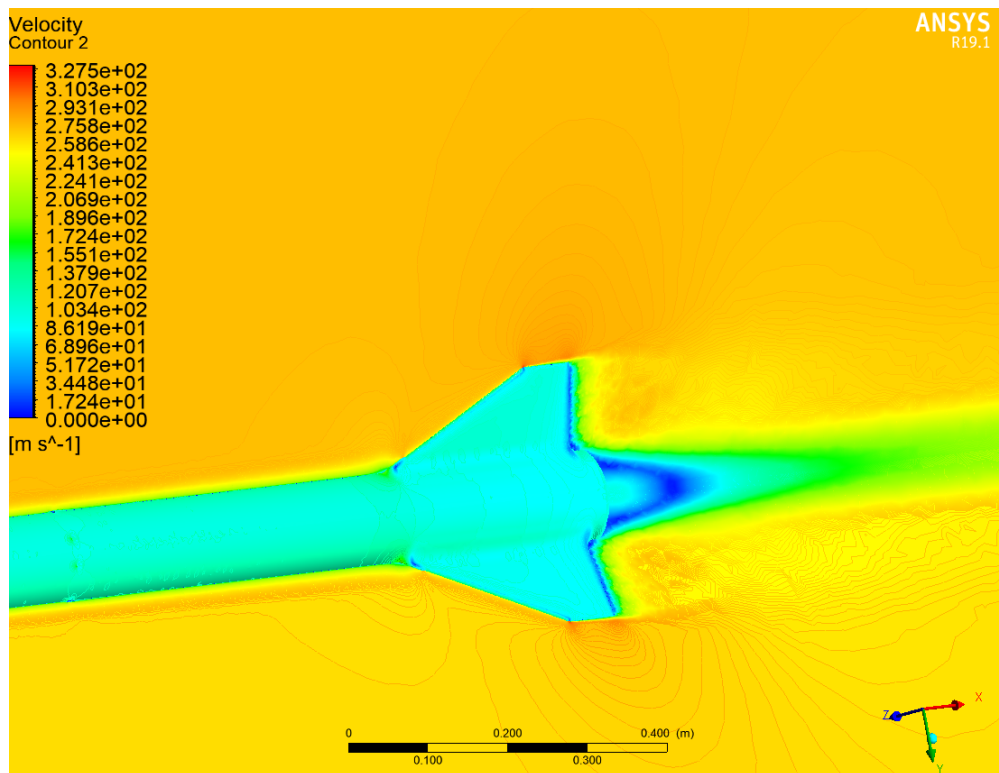
Figure 39   Flow at Mach 0.8 over the fins

We are also starting to look into fluid-structure interaction which is a coupled analysis between CFD and FEA. The idea is to model the fluid flow over the fins and use the pressure data to analyze bending and vibration in the fins. This will be complementary to the fin flutter analysis that we have been trying to perform. As fins are a critical part of a rocket, it is essential to know how the fins will behave during flight to avoid reaching resonant frequencies or static failure. Especially since the Base 11 rocket will be undergoing high velocities and pressures, being able to predict how the flow deforms the fins will be a useful asset.

J. Flight Dynamics

In order to ensure the stability of the rocket during flight, we will include in our simulations an estimation of the Rocket's stability by use of the Barrowman equations defining the position of the center of pressure relative to the nosecone tip:

$$\bar{X} = \frac{C_N X_N + C_T X_T + C_F X_F}{C_N + C_T + C_F}$$

Each of these coefficients will be calculated following the work of Barrowman in [7]. This allows the approximate determination of the center of pressure during sub- and super-sonic flight, though further research must be done into the effects of transonic flight on the validity of Barrowman's estimate, though the vehicle spends little time in the transonic region. The center of gravity will be determined from the CAD model of the rocket. Knowing both the CP and CG allows for an estimate of the static stability of the rocket (i.e. the ability of the rocket to generate restoring aerodynamic moments when deviating from the flight axis).

Another design consideration is the stability of the rocket off-the-pad. While fairly large ranges of stability are acceptable in flight, it is desirable to maintain precise control over the vehicle as it leaves the pad to prevent propagation of errors through the whole flight-path. To this end we seek to limit the Stability ratio (the distance from CG to CP divided by vehicle diameter) to be approximately 1.5 - 2.

Though an estimate of the passive stability of the rocket is of great value, it is has also been deemed necessary to maintain some degree of active control during flight. The development of active control systems serves three primary purposes: to counteract the negative effects of passive stability (e.g. weathercocking), to ameliorate the influence of small perturbations on flight, and to minimise the effects of dynamic stability. As such, a number of methods of active control have been considered. Thrust vectoring would allow for improved control over the moments affecting flight. In order to reduce rolling moments, CO_2 reaction thrusters have been proposed. Actuated fins are another option under consideration.

In all cases, the complexity of active control is considerable. To aid the design process, accommodation of active control elements has been made a design goal of the simulator software under development (which also accounts for passive, aerodynamic control effects). Active control also requires integration of the associated sensors and actuators with the flight computer.

K. Electronics - Hardware

1. Flight Computer Subsystem Overview

For the Rocket System portion of the SLS to be space capable, a robust flight computer capable of performing several tasks simultaneously is required. The flight computer system fulfills requirements 1, 5 and 6 of the overall Rocket System. These requirements are herein reiterated as:

1) The rocket shall reach an altitude of 100 km.
2) The rocket shall be fully recoverable.
3) The rocket shall maintain in flight stability.

To fulfill the above-mentioned requirements, system specific requirements are placed upon the flight computer itself, independent of all other subsystems of the rocket. These requirements are herein stated as:

1) The Flight Computer shall sustain a communication link to ground at all stages of operation.
2) The Flight Computer shall be fully autonomous in flight.
3) The Flight Computer shall be, at minimum, doubly redundant.
4) The Flight Computer shall be powered on and off remotely.
5) The Flight Computer shall fail electrically off.
6) The Flight Computer shall interface with Avionics Bay.

Flight Computer System requirement 1 allows a direct feed of information from the rocket to Mission Control to give Mission Control personnel situation awareness of the rocket, its state and its environment at all phases of the mission.

This requirement is critical in fulfilling Rocket System requirement 1.

Flight Computer System requirement 2 directly fulfils Rocket System requirement 3 and eliminates the possibility of flight instability due to human error (e.g. accidental false information feed from ground to rocket).

Flight Computer System requirement directly fulfills Rocket System requirement 2 and 3. It mitigates the possibility of flight instability and mission failure by minimizing single points of failure with the overall flight computer system through a minimum of double redundancy.

Flight Computer System requirement 4 is a safety specific requirement that implements overall SLS and personnel safety, especially when the SLS is in a hazardous state.

Flight Computer System requirement 5 implements safety and indirectly implements Rocket System requirement 2. The Flight Computer System failing electrically off allows the Rocket System to continue flight on its inherent stability and mitigates the possibility of erroneous decision being made by the Process and Control Center due to failure.

Flight Computer System requirement 6 is an assembly specific requirement.

The current flight computer subsystem is further segregated into four blocks and their respective sub-blocks. These four blocks are as follows (See Figure 40 for further details).

- Process and Control Center
- Instrumentation Suite
- Telemetry Block
- Power Block

The Process and Control Center acts as the main brain for the entire flight computer system. This is where information (about the rocket, its state and its environment) is processed and used in autonomous decision making. The Instrumentation Suite constitutes all the sensors (both internal and external) used to gather information about the rocket, it's state and its environment. The Telemetry Block handles wireless downlink communications with Mission Control. Finally, the Power Block orchestrates power distribution from external and internal rocket power to all the above-mentioned blocks of the flight computer.
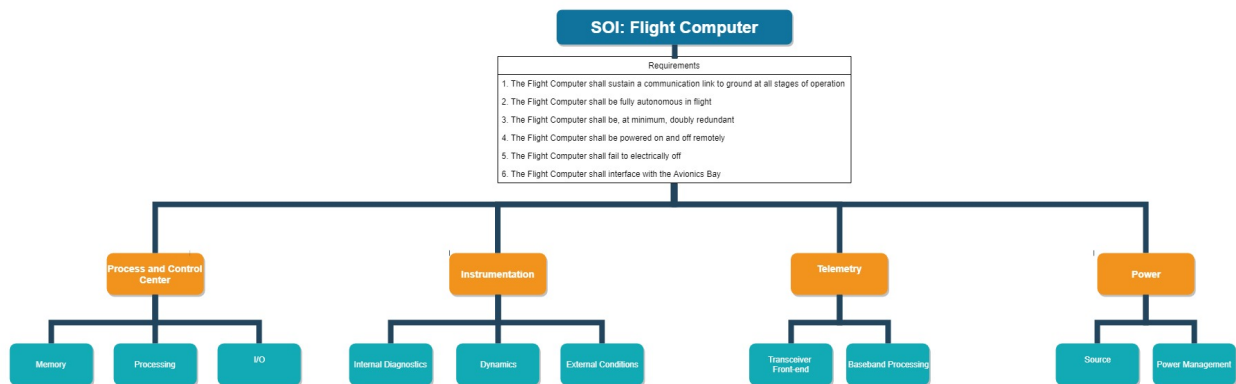
Figure 40   Flight Computer System architecture.

2. Power Block

II.K.2.1   Overview   As stated, the Power Block of the Flight Computer System directly handles power management and power source for all the electronics encompassed within the Flight Computer System. The Power Block can be separated into two sub-blocks: Power Source and Power Management (See Figure 41). The Power Block directly fulfills Flight Computer System requirement 3, 4 and 5. It indirectly implements all the other requirements by support of other sub-blocks within the Flight Computer System. Direct fulfillment of requirements 3, 4 and 5 are discussed within the

Section 1.2.2. To fulfill a minimum of double redundancy, there are to be two fully independent Power Blocks within the Flight Computer System.

Figure 41   Power Block architecture.

II.K.2.2   Architecture

II.K.2.2.1   Source   The Source sub-block of the Power Block consists solely of the power source and internal supporting electronics (i.e. impedance matching electronics for maximum power delivery to the Power Management Block). The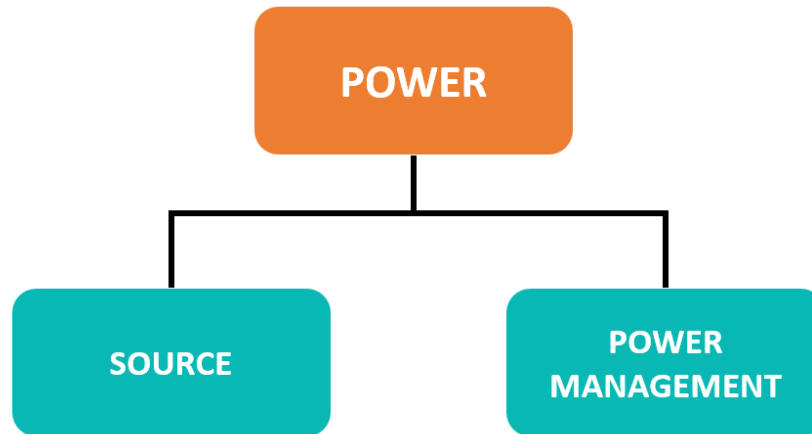 obvious choice for the power source is an electro-chemical battery with a charge capacity capable of sustaining all the electronics with power for a minimum duration of at least twice the duration of the mission duration – from power on state (i.e. first flow of electrical power) to complete power off state (i.e. no electrical power flow anywhere). To mitigate single points of failure each Power Block is to have two fully independent Source sub-blocks.

II.K.2.2.2   Power Management   The Power Management sub-block of the Power Block consists of all the electronics in charge of handling, modifying and regulating the flow of power. The Power Management sub-block follows a, here-in named, "Nexus" architecture (See Figure 42). The remainder of this section will describe the Power Nexus architecture.

The Power Nexus (here-after referred to as "the nexus") is the primary module of the Power Management sub-block. The primary function of the nexus is regulation and routing of internal and external power. The entire nexus is run by a power management controller. The controller monitors and controls all power regulation, recycler and dump sections. Electrical information (e.g. incoming/outgoing current levels, voltage levels) are used in power relevant computations (e.g. monitoring over current faults, over voltage faults, internal power source life remaining). The power management controller also has an uplink wireless communication line (green in Figure 3) for remote power-on and power-off capability. The power management controller also has a bidirectional communication line (yellow in Figure 3) to the Process and Control Center Block of the Flight Controller System. This communication line is in place to share information with the Process and Control Center. One case would be warning the Process and Control Center of an imminent power-off to avoid unintentional corruption of data due to an abrupt disconnection of power. Another case would be allowing the Process and Control Center to notify the power management controller of a problem downstream. In this case the power management controller would shut off power to the problem unit. (Aside: The power-down routine of the Process and Control Center Block is described within Section 2.3.2.2).
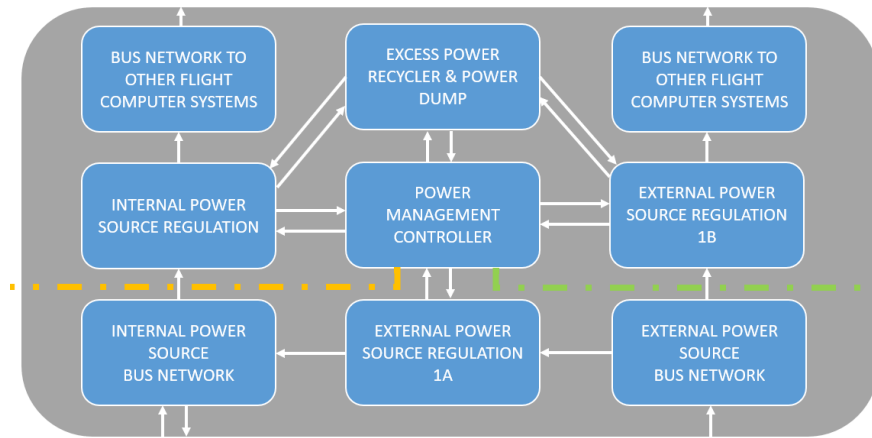
Figure 42   Power management nexus architecture.

The internal power source bus network implements impedance matching for maximum power transfer between the internal power source (Source on-board the rocket) and relevant regulation sections. The external power source bus network functions in the same way, except it is used for the external power source (power source coming from launch pad). To mitigate single points of failure, there are multiple bus lines within the bus networks.

The external power source regulation sections (both 1A and 1B variant) are used to regulate and control power flowing in from the external power source bus network. The external power source regulation section is also capable of completely inhibiting power flow from the external power source bus network by making use of soft and hard electrical disconnects. The difference between regulation section 1A and 1B is the additional electrical elements in 1A to facilitate charging of the internal power source while the external power source is connected and when necessary.

The internal power source regulation sections are used to regulate and control power flowing in from the internal power source bus network. The internal power source regulation section is also capable of completely inhibiting power flow from the internal power source bus network by making use of soft and hard electrical disconnects (e.g. transistor switches, relays, fuses).

The excess power recycler and power dump section is responsible for dissipating or recycling excess power. Rather than initiate a total and complete hard disconnection from power sources during over current or over voltage situations, which would power-off other subsystems of the flight computer, the excess power will be directed towards the power recycler and power dump section. This section will initially attempt to store the excess power to be redistributed back into the power regulator sections. In the case where the storage is at capacity, the remaining current and/or voltage is dumped and dissipated. To prevent backflow of power back into the system in the power-off state, any stored energy is dumped before the power management controller powers down.

Finally, the bus networks to other flight computer systems on the internal and external power source lanes of the nexus are essentially the same. These sections are simply the collection of transmission lines that deliver power to the other Flight Computer System blocks.

3. Instrumentation Suite

II.K.3.1   Overview   The Instrumentation Suite houses all the transducers and sensors that collect data on various aspects of the rocket. The collected data is immediately sent to the Process and Control Center for processing. The instrumentation suite can be broken down into three sub-blocks (See Figure 43).
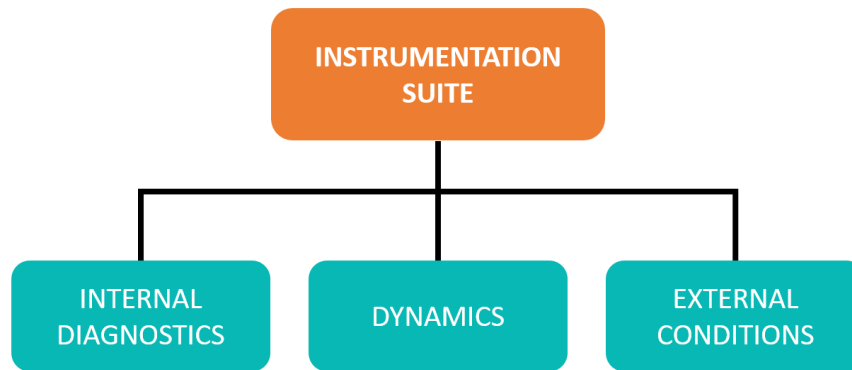
Figure 43   Power management nexus architecture.

The internal diagnostics sub-block constitutes all the sensors, transducers and supporting electronics used to diagnose the conditions within the rocket airframe. The dynamics sub-block constitutes all the sensors, transducers and supporting electronics used to collect data on the dynamics of the rocket system. The external conditions sub-block constitutes all the sensors, transducers and supporting electronics used to monitor the environment the rocket is situated in.

The Instrumentation Suite directly implements Flight Computer System requirements 3 and 5. Instrumentation supports the Process and Control Center in implementing Flight Controller System requirement 4. To fulfill double redundancy, sensors and the individual sub-blocks are duplicated.

II.K.3.2   Architecture

II.K.3.2.1   Internal Diagnostics   The internal diagnostics sub-block of the Instrumentation Suite incorporates sensors and transducers used to collect data on the internal environment within the airframe and the airframe itself. The suite sensors and transducers included in the internal diagnostics sub-block are listed below.

- Barometric Pressure Sensor
    - Collect data on atmospheric pressure within the rocket.
- Temperature Sensor
    - Collect data on temperature within the rocket.
- Humidity Sensor
    - Collect data on the humidity within the rocket.
- Photovoltaic Sensor
    - Collect data on optical intensity within the rocket.
- Thermocouple
    - Placed against the skin of the airframe on the inside to collect interior airframe skin temperature.

Most of the sensors and transducers on the list are self-explanatory. The two that require further discussion are the photovoltaic sensor.

Photovoltaic sensors can in various variants for different optical wavelengths. Photovoltaic sensors for visible light can be used to confirm separation of the rocket for deploying the recovery mechanism or the payload. They can also be used, in tandem with other sensors, to detect a possible airframe rupture on the rocket. UV photovoltaic sensors can also be used to monitor how well the interior of the rocket is being shielded from low energy radiation.

The sensors and transducers on the same board within the internal diagnostics sub-block incorporate a small data acquisition suite to help synchronize and facilitate data transfer between the Process and Control Center and the sensors. This data acquisition suite constitutes microcontroller and amplification electronics for the relatively weak electrical signals from transducers.

The data acquired from the internal diagnostics sub-block is used by the Process and Control Center to monitor the internal environment within the rocket system. Should any sensors and/or transducers record measurements beyond permissible limits, the Process and Control Center raises an alarm that is eventually transmitted to mission control. In addition to this, commands are sent to the appropriate controllers to attempt to reconcile the off-nominal reading by checking it against redundant sensors within the same general area. Should the sensor be deemed continuously erroneous in data readings, the Process and Control Center bypasses the sensor or transducer.

II.K.3.2.2 Dynamics The dynamics sub-block of the Instrumentation Suite incorporates sensors and transducers used to collect data on the dynamics of the rocket system. The suite of sensors and transducers used are listed below.

- Accelerometer
  - Collects data on acceleration of rocket in space. From this other information such as position, velocity, attitude and spatial vibration modes of the rocket system can be derived.
- GPS Module
  - Collect data on longitude and latitude position of rocket, as well as altitude of rocket. *
- Gyroscope
  - Collect data on the orientation and rotation of the rocket system.
- Magnetometer
  - Collect data on heading and bearing of rocket system.
- Thermocouple
  - Collect data on temperature within engine block to deduce quality and level of combustion.
- Piezoelectric Strain Gauges
  - Collect data on strain modes present within the airframe of the rocket.

* Note: Commercial GPS modules lock out above a specific altitude. GPS will only be useful while the rocket is below the lockout altitude.

The sensors and transducers on the same board within the internal diagnostics sub-block incorporate a small data acquisition suite to help synchronize and facilitate data transfer between the Process and Control Center and the sensors. This data acquisition suite constitutes microcontroller and amplification electronics for the relatively weak electrical signals from transducers.

The data acquired from the dynamics sub-block is used by the Process and Control Center to monitor the dynamics of the rocket system. Should any sensors and/or transducers record measurements beyond permissible limits, the Process and Control Center raises an alarm that is eventually transmitted to mission control. In addition to this, commands are sent to the appropriate controllers to attempt to reconcile the off-nominal reading by checking it against redundant sensors within the same general area. Should the sensor be deemed continuously erroneous in data readings, the Process and Control Center bypasses the sensor or transducer.

II.K.3.2.3 External Conditions The external conditions sub-block of the Instrumentation Suite incorporates sensors and transducers used to collect data on the state of the external environment surrounding the rocket system. The suite of sensors and transducers used are listed below.

- Barometric Pressure Sensor
  - Collect data on atmospheric pressure outside the rocket.
- Temperature Sensor
  - Collect data on temperature outside the rocket.
- Humidity Sensor
  - Collect data on the humidity outside the rocket.
- Camera
  - Capture and store footage of exterior of rocket.
- Thermocouple
  - Placed against the skin of the airframe from the inside to collect exterior airframe skin temperature.

The sensors and transducers on the same board within the internal diagnostics sub-block incorporate a small data acquisition suite to help synchronize and facilitate data transfer between the Process and Control Center and the sensors. This data acquisition suite constitutes microcontroller and amplification electronics for the relatively weak electrical signals from transducers.

The data acquired from the external conditions sub-block is used by the Process and Control Center to monitor the external environment the rocket system is surrounded by. Should any sensors and/or transducers record measurements beyond permissible limits, the Process and Control Center raises an alarm that is eventually transmitted to mission control. In addition to this, commands are sent to the appropriate controllers to attempt to reconcile the off-nominal reading by checking it against redundant sensors within the same general area. Should the sensor be deemed continuously erroneous in data readings, the Process and Control Center bypasses the sensor or transducer.

4. Processing and Control Center

II.K.4.1 Overview   The Process and Control Center is the core block of the Flight Computer System and is responsible for collecting data from other Flight Computer System blocks, processing the data, making a decision, formulating a command based on that decision and sending that command to other Flight Computer System blocks. The Process and Control Center can be separated into three sub-blocks: Memory, Processing, Input/output (See Figure 44).

The Process and Control Center directly fulfills Flight Computer system requirements 2, 3, and 5. It indirectly implements all other requirements by support of other sub-blocks within the Flight Computer System. Direct fulfillment of requirements 2, 3, and 5 are discussed within Section 1.3.2. The memory sub-block is paired with each processing block. Each processing block is connected to an input-output sub-block. These pairings are then duplicated to fulfill a minimum of double redundancy.
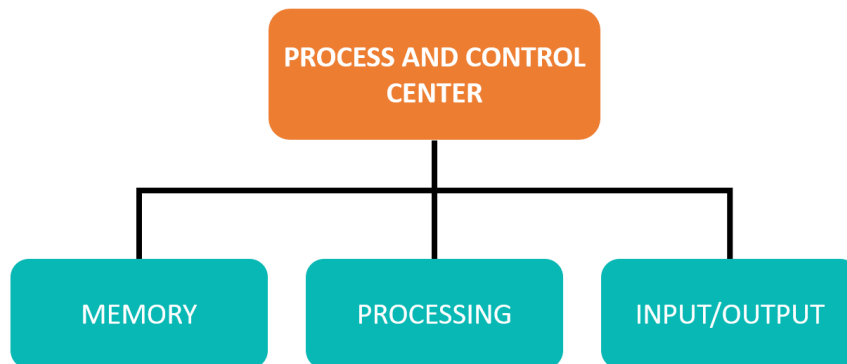

Figure 44   Process and Control Center.

II.K.4.2   Architecture

II.K.4.2.1   Memory   The Memory sub-block of the Process and Control Center consists solely of all information storage units and supporting electronics. This includes both permanent and temporary information storage mediums. These mediums will store information about the rocket system, its state and environment from initial power-on to power-down of the Process and Control Center. Information stored within permanent storage remains there until deleted. Information stored in temporary storage is erased at power-down and cannot be recovered once lost.

Temporary information storage mediums, such as cache and RAM, are usually faster to read from and write to, in comparison with permanent information storage mediums. On the other hand, permanent information storage mediums are several orders of magnitude larger than temporary information storage mediums in terms of capacity. Therefore, temporary information storage mediums are to be used to store intermediate results for computations done by the

processing sub-block. Whereas, permanent storage will be used as a mission log for the rocket system, its state and the state its environment.

II.K.4.2.2 Processing   The processing sub-block of the Process and Control Center consists of all electronics required for taking in data from other blocks, decision making based on this data, command formulation and communication of these command to other blocks within the Flight Computer System or the Rocket System. The result of this taking a rocket from a nominal or an off-nominal state to a nominal state. The easiest example of a command would be one sent from the Processing block to the engine controller. This command could range from engine-shutoff to thrust vectoring actuation. Attitude, altitude, position, instrumentation, environment and engine monitoring all occur within this block.

At the core of the processing sub-block is a microcontroller. This microcontroller is capable of reading and writing to its partner memory sub-block and input/output (herein abbreviated I/O) ports. This microcontroller is also capable of communicating directly with microcontrollers within other processing sub-blocks. The reason for this feature is to allow processing sub-blocks to share and compare information. This architecture serves to mitigate erroneous decisions derived from computational error. The processing sub-block also consists of support electronic elements to assist the microcontroller. These include (but are not limited to) signal regulators, signal matching networks, signal multiplexers etc.

To implement an electrically off failure mode, the processing block has a communication link to the power management block of the Power Block.

II.K.4.2.3 Input and Output   The I/O sub-block of the Process and Control Center is a network of bus wires used for interfacing the processing sub-block with Flight Computer System blocks, other subsystems within the rocket and additional peripherals. Excluding microcontroller-to-microcontroller communication, any information coming in or leaving the Process and Control Center passes through this sub-block.

The I/O sub-block is made up of the primary bus wires for communications protocols used by the processing sub-block and other supporting electronics. The I/O sub-block also contains standardized terminals for these bus wires to allow easy interfacing with electrical connectors.

5. Telemetry Block

II.K.5.1 Overview   The Telemetry Block is responsible for maintaining a constant downlink communication with mission control on the ground. This downlink communication allows the rocket to send real-time information to mission control, where it is used to increase personnel situation awareness of the mission. The Telemetry Block can be subdivided into two sub-blocks (See Figure 45).
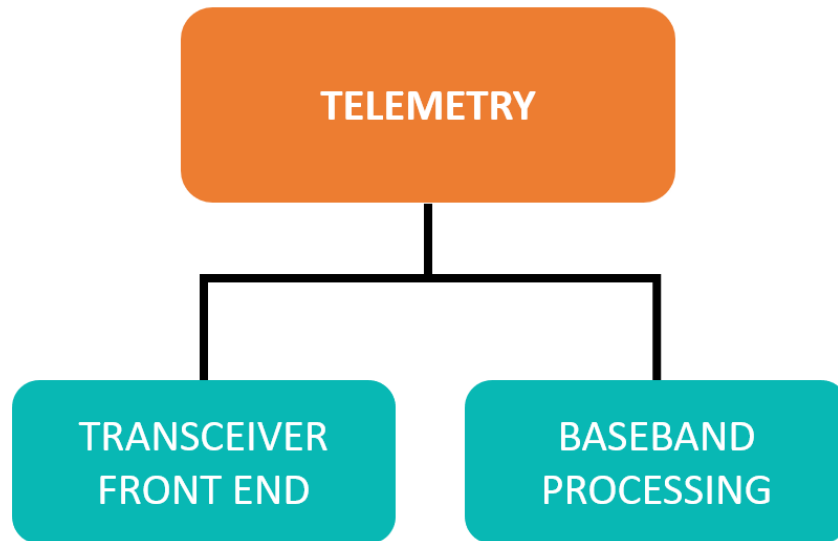
Figure 45   Telemetry Block architecture.

The transceiver front-end sub-block acquires the raw incoming analog signal and converts it into a baseband signal that can be manipulated by the baseband processing sub-block. Or, in the reverse process, the transceiver front-end sub-block takes a baseband analog signal from the baseband processing sub-block and modulates it to a transmittable signal. The baseband processing sub-block extracts information from the converted analog signal coming from the transceiver front-end. Or, in the reverse process, the baseband processing sub-block encodes information into an analog signal that is then fed to the transceiver front-end.

The Telemetry Block directly implements Flight Computer System requirement 1 and acts as a backup for requirement 4. To fulfill double redundancy, the transceiver front-end and baseband processing sub-blocks are duplicated.

II.K.5.2   Architecture

II.K.5.2.1   Transceiver Front-End   The transceiver front-end of the Telemetry Block consists of all non-baseband processing electronic elements that are used in reception/transmission, demodulation/modulation, down/up-conversion, filtering and amplification of raw analog signals. To perform this operation the transceiver front end makes use of an antenna, low noise amplifiers, filters, mixers and oscillators. The arrangement of these elements depends heavily on the transceiver architecture chose. There are as many architectures of transceivers as there are configurations of the elements within them.

The transceiver front-end is a passive as it does not require a controller to function. The output of the transceiver front-end is fed directly into the baseband processing sub-block.

II.K.5.2.2   Baseband Processing   The baseband processing sub-block of the Telemetry Block consists of all active processing electronic elements used to convert a baseband analog signal into digital data that can be manipulated by controllers and the Process and Control Center. The baseband processing block also performs the reverse operation, wherein it converts a digital signal into a baseband analog signal fit for modulation and subsequently transmission. The baseband processing block achieves these conversions by means of an Analog-to-Digital converter.

The other main component within the baseband processing block is a microcontroller that synchronizes and facilitates digital data transfer between the Processing and Control Center and the Telemetry Block. In the case of failure within the Process and Control Center, this microcontroller transmits a predetermined error message to mission control to alert personnel of lack of input from the Processing and Control Center.

53

Other constituents of the baseband processor depend on the specific architecture of baseband processing chosen. There exists and endless list of various architectures.

L. Electronics - Software

1. Overview

The main software running on the Flight Computer Subsystem of the Rocket System portion of the overall SLS is a real-time operating system. This software is to be installed on the microcontroller units within the Processing and Control Center Block.

A stripped-down version of this real-time operating system is to be installed on the microcontrollers that aid other blocks within the Flight Computer Subsystem to communicate clearly and coherently with the Process and Control Center Block. This stripped-down version does not include memory management or file system management.

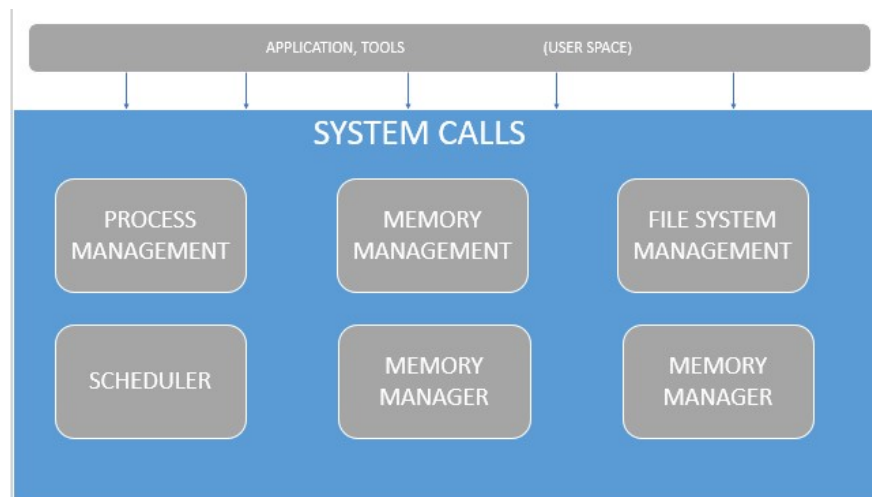The architecture for the real-time operating system can be seen in Figure 46.

Figure 46   Real-time operating system architecture

2. Applications

Applications are the highest-level process running within the operating system. These programs are written for independent tasks to be completed by the microcontroller on which they are installed. Applications abstract away the physical nature of the hardware in use and are concerned only about the high-level sequential order in which the hardware is used. Most of the routines running on the rocket, from engine monitoring to Process and Control Center command execution are applications. Due to the multithreading capabilities of the real-time operating system, applications running on a single microcontroller can be executed simultaneously. This allows something like the engine to be throttled, while simultaneously monitoring the engine output to ensure it is on track. Filtering sensor data, processing, decision formulation and command execution are all applications.

3. Process Management

The process management is a level lower than the applications. This software manages all the applications running, making sure that critical hardware resources are available to applications when they are required. The process management ensures that critical hardware resources are not being hogged by a single application. Critical resources could be CPU computation time, a physical CPU core, cache memory, RAM etc. The process management also works to mitigate deadlock situations. All in all, the process management ensures that applications run as smoothly as possible. The implementation of process management is the scheduler. This implementation schedules instructions from various processes and instructs the CPU on which operation to execute and when.

4. Memory and File System Management

The memory management, implemented by the memory manager, controls and coordinates the memory allocated to the various processes. It is the job of memory management code to ensure that memory blocks allocated to various processes, especially within temporary storage, do not collide. In the case of a collision, one process might overwrite critical data from needed for another process, ultimately leading to an error within memory. It is also the job of memory management to ensure that the blocks of memory allocated are adequately sized for the needs of the application. The memory manager allocates memory upon request from the application.

File system management is a superset of memory management. File system management only occurs within permanent information storage mediums. The file systems management is also implemented by the memory manager. File systems management involves organizing stored information into sorted directories, so as to optimize the retrieval of this information at a later time.

M. Recovery System

1. Recovery Overview

The recovery phase of the flight consists of a dual separation and a dual deployment. The first separation occurs at an altitude of about 30 km. The separation point is near the middle of the airframe, at the tube separation above the engine. The first event deploys the drogue parachute. The second separation deploys the main parachute and occurs at an altitude of 1500 m, which gives the parachute just enough time to fully open while minimizing the effects of wind drift. The separation point is at the bottom of the nose cone. Both separations are achieved with the same mechanism involving pressurized carbon dioxide. Note that the diagram shown in 47 is not to scale.

Figure 47   Deployment Sequence

2. Structural Integrity

At each point of separation, one side of the coupler is attached to the body tube or nose cone with nylon screws which serve as shear pins. Shear pins ensure that the airframe stays together for as long as needed until it needs to separate, at which point the shear pins are prescribed to break upon a certain applied force. Since the ejection chambers need to remain as airtight as possible in order to minimize leaks during the pressure buildup for separation, there are no vent holes in them. As a result, the nylon screws need to be strong enough to resist the forces caused by the changes in atmospheric pressure due to the rocket moving from sea level up to 100 km in altitude. At the Karman line, the atmospheric pressure is negligible. As a result, assuming a pressure differential of 14.7 psi and an airframe diameter of 14 inches, fourteen $1/2 - 20$ nylon screws are needed, which give a safety factor of 2.0.

3. Separation Mechanism

Black powder ejection is traditionally the most effective and reliable method to separate rocket sections. However, as the altitude increases, the atmospheric pressure and air density considerably decrease. As a result, at higher altitudes,

full combustion of black powder cannot be guaranteed, as there is very little medium for heat transfer to occur between all the particles. It is therefore critical to contain the black powder within a charge well with minimal volume to ensure that all particles are in contact with one another. The charge well must also be able to contain the combustion for as long as possible. If the charge well releases the pressure prematurely when only a fraction of particles is combusted, the remaining particles will be sucked away due to the lower atmospheric pressure, resulting in incomplete combustion. The charge well must nonetheless be able to release the pressure created by whatever amount of black powder it holds.

Due to large size of the rocket, if we choose to solely use the combustion of black powder to pressurize the ejection chamber, we would need a large amount of it. Assuming a chamber volume of 460 sq. in., i.e. a 3-inch tube length, 10 grams of 4F black powder is needed per charge well to break the nylon screws with a safety factor 1.8. The full combustion of 10 grams of black powder inside a charge well of minimal volume would cause an extreme pressure buildup that would be very challenging to contain properly, especially since the pressure ultimately still needs to be released into the ejection chamber.

Due to this complication, we are instead opting for compressed CO_2 to build up pressure inside the ejection chamber. Assuming the same chamber volume of 460 sq. in., 50 grams of CO_2 delivers enough pressure for the nylon screws to break, with a safety factor of 2.0. For redundancy, two 50-gram cartridges are needed. The CO_2 ejection system consists of a compressed gas cartridge, a spring, a hollow thumbscrew, a puncturing piston, and a flanged housing which serves to secure the setup onto a bulk plate. Only about 0.5 gram of black powder is to push the piston so that it punctures the cartridge. The base of the piston rests against the hollow thumbscrew which holds the black powder. The housing has multiple vent holes so that the CO_2 may escape into the ejection chamber once the cartridge is pierced. See Fig. B. The housing is designed such that the vent holes are on the opposite side of the bulk plate to the body of the gas cartridge, to allow for a smaller chamber volume. It is important to note that since the pressurization will not occur as instantaneously as with black powder, it is crucial that the ejection chamber is airtight.

The resulting ejection shock force, which needs to be sustained by the recovery harness and the parachutes, assuming that both CO_2 cartridges successfully puncture, is 7000 lbs. This number would be more accurate for a black powder ejection, since it happens more quickly. With CO_2 cartridges, the release of gas is slightly more gradual, which means that the tubes may be able to separate before all of it is released. In this scenario, the shock force would be considerably lower than 7000 lbs.
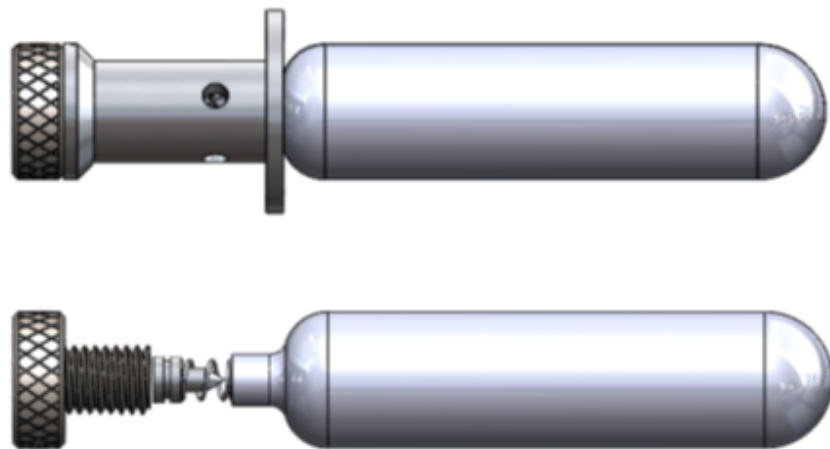

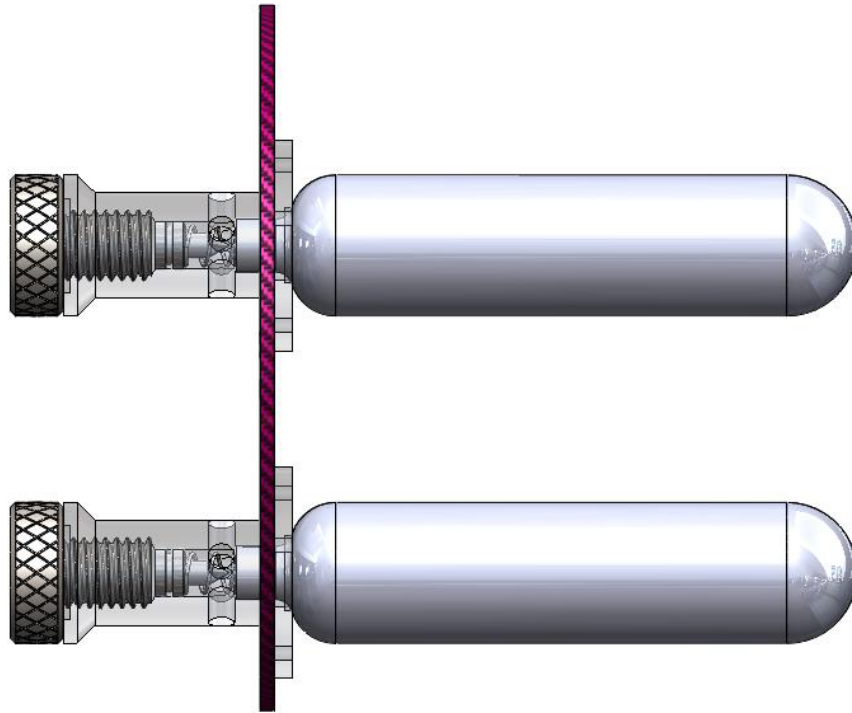**Figure 48   Carbon Dioxide Ejection Mechanism**

Figure 49   Carbon Dioxide Ejection Mechanism Mounted on a Bulk Plate

4. Parachutes

The timing of the first parachute deployment is challenging to optimize. Parachutes are able to provide more drag, which may only be created if there is a fluid around, i.e. air. Therefore, the first deployment cannot occur near apogee, because there is practically no air at that altitude ($5.6x10^7 kg/m^3$ or $3.5x10^8 lb/ft^3$). As a result, the parachute simply would not be able to open. It is also worth noting that in thinner air, the effects of ejection are amplified and the terminal velocity is much higher due to the lack of air resistance. With this in mind, we must wait until the rocket is gradually slowed down by the thickening atmosphere as it falls. To provide more context, 99.9 % of the atmosphere lies below the mesosphere, i.e. below the stratopause at 50 km, which is half of the target apogee. It is therefore highly unlikely that a parachute will be able to open at altitudes higher than 50 km. Since there is very little literature on the minimum air density needed for a parachute to properly open, testing will be required.

The goal when determining an adequate deployment altitude is to find one at which the parachute opening force is lowest. The parachute opening shock is calculated using a program called OSCALC (see 50), developed by the Parks College Parachute Research Group. This program has been used in the past for other projects, and results have always agreed with other literature. Input values include the atmospheric density at deployment, the mass of the rocket, the speed of the rocket at deployment, the Cd of the parachute, the area of the parachute, the parachute opening time, and a theoretical opening shock factor. The estimated speed of the rocket at deployment is obtained with the terminal velocity equation.

$$V_{term} = \sqrt{\frac{2W}{C_d \rho A}}$$

Figure 50   Screen capture of the OSCALC program

The advantage of deploying a parachute at higher altitudes is the fact that the lower air density causes a slower opening time, given that the parachute is able to open, resulting in a lower opening force. However, a higher altitude deployment also means that the velocity of the rocket at deployment is much higher, which in turn increases the opening shock force. Multiple iterations considering different deployment altitudes were run in OSCALC (see Table A). We may notice that the parachute opening shock force, for any altitude between 50 000 and 250 000 ft, falls around 2500 lb. From these results, we know that the deployment may be set at any altitude within that range, given that the parachute is able to open.

The drogue deployment is currently set at 100 000 ft, but is subject to change depending on test results determining the minimum air density required for a parachute to open. The main parachute is set to deploy at about 5000 ft. Both parachutes deploy as a result of the separation, so the two separations occur at the same respective altitudes.

Both parachutes will be of semi-ellipsoidal shape, with a 20% diameter vent hole. This parachute shape has been manufactured and tested in the past, so we know that its Cd is 1.6. Higher drag coefficients provide a better drag-to-diameter ratio, but considerably increases the parachute opening shock force because the opening time is typically shorter. The canopy will be made of 1.6 oz zero-porosity ripstop nylon. Currently, our design calls for a 48-inch-diameter, semi-ellipsoidal drogue parachute, which provides a terminal speed of a little under 150 ft/s when the main deployment needs to occur. The 228-inch-diameter, semi-ellipsoidal main parachute provides a terminal descent speed of a little under 29 ft/s. The main parachute has an opening shock force of 2566 lbs. Considering both the ejection shock force and the opening shock force, both parachutes should be designed to handle at least 20 000 lbs for a safety factor of above 2. As such, we will be using the 1000-lb-break Microline as suspension lines, and will have 20 of them on each parachute. It is worth noting that the recovery harness (next section) should be able to handle that same 20 000 lbs of force.

5. Recovery Harness

Following each separation, a recovery harness connects all components, in order to facilitate the recovery of the rocket once it hits the ground. Also, this way, only one set of electronics is needed. The recovery harness refers to all shock cords and hardware such as eyebolts and quick links. These components need to be strong enough to absorb most of the energy resulting from ejection and from parachute deployment.

Due to the high strength required by these components, the harness needs to be split into multiple sections in parallel. In other words, instead of having a single shock cord attached to one eyebolt on each end, we would have multiple shock cords independently attached to their eyebolts. This approach reduces stress concentrations on the bulk plate to which the eyebolt would be attached, by having multiple eyebolts instead, distributing the load. Another advantage of this method is the possibility of having "consumable" shock cords, i.e. shock cords which are designed to break once it absorbs enough energy. For instance, if we implement three cords in parallel, we may manufacture them to different lengths, so that the first cord that becomes taut takes the ejection load, and is designed to break as a result. Then, the second cord that becomes taut will take the remaining load, and so on for the third cord. Since some of the energy is dissipated through the consumable cords, there will be much less stress on the bulk plate and eyebolts, provided that they have higher strength ratings than the cord.

The shock cords will be manufactured using tubular Kevlar, chosen for its high tensile strength and minimal elasticity. Elastic shock cords should be avoided as the energy they build up will result in the rocket components smashing against one another following separation. Loops will be sewn at each end using nylon thread, as knots considerably weaken the cord.

N. Ground Support Equipment

1. Ground Computer

Data collected from sensors onboard the rocket is continuously transmitted to, and received on the ground station. The ground station saves and plots flight data in real-time, in order to track the position of the rocket and estimate performance. The software, which can currently be run on any laptop, is programmed in Python, and displays performance indicators from the flight, to the user, with Tkinter.

The user interface displays five key graphs: temperature (°C), altitude (m), velocity (m/s), acceleration (m/s^2), and GPS location (latitude vs. longitude). Flight data from the rocket is read from the receiver attached the the ground station. These strings are then parsed, and the appropriate values are extracted, saved, and plotted. The points on the GPS plot (UTM coordinates) are color coded in a gradient from blue (lowest altitude) to red (highest altitude), with the most recent coordinate in white. This helps easily identify and evaluate the rocket's trajectory.
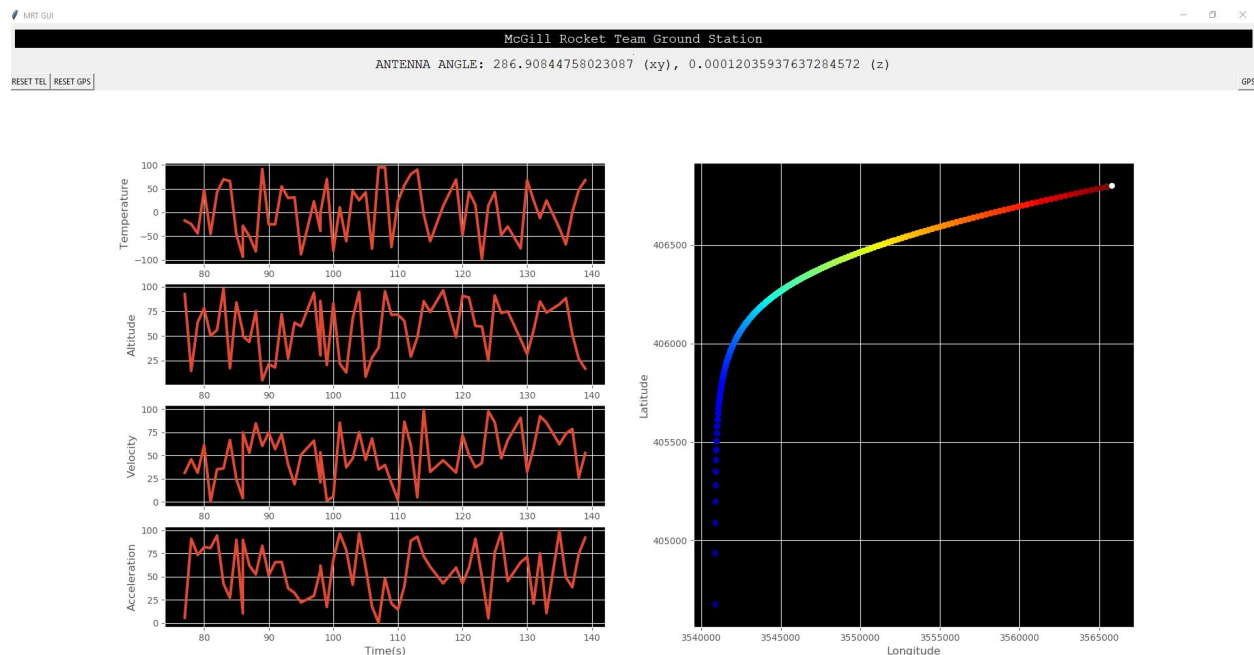
Figure 51   Ground Computer GUI

Although all flight data is displayed on the graphical user interface (Figure 51), it is also saved to the file system on the ground station. These files, organized by date and time, ensure that all received information is stored and accessible for future analysis. This is essential because it offers the possibility to look back at previous launches or test runs to evaluate the performance of the rocket, and increases possibility for improvements.

In order to obtain the best signal strength from the telemetry circuits, the antennas on the ground station must be pointed toward the rocket during flight. As the rocket's height increases, it becomes harder and harder to track its approximate location with the naked eye. Since the latitude, longitude, and altitude of the ground station are known, and since the latitude, longitude, and altitude of the rocket are obtained, the relative angle of the rocket to the ground station in the xy and z-plane can be calculated. These values are displayed on the GUI and can be used to direct the antennas in the proper direction.

The nature of the Base 11 challenge could pose some future problems for the ground station. A longer flight time would mean that the software would have to be run for an extensive amount of time, while saving and displaying large amounts of data. It is essential that the software is as reliable, robust, and lightweight as possible to account for this. Since sensors onboard the rocket may break or malfunction at such high altitudes, the internal parser of the ground station must be sophisticated enough to recognize and deal with this, without affecting the rest of the received data. A trajectory projection feature is also being discussed so that the location of the rocket can be estimated in the event of a GPS sensor malfunction.
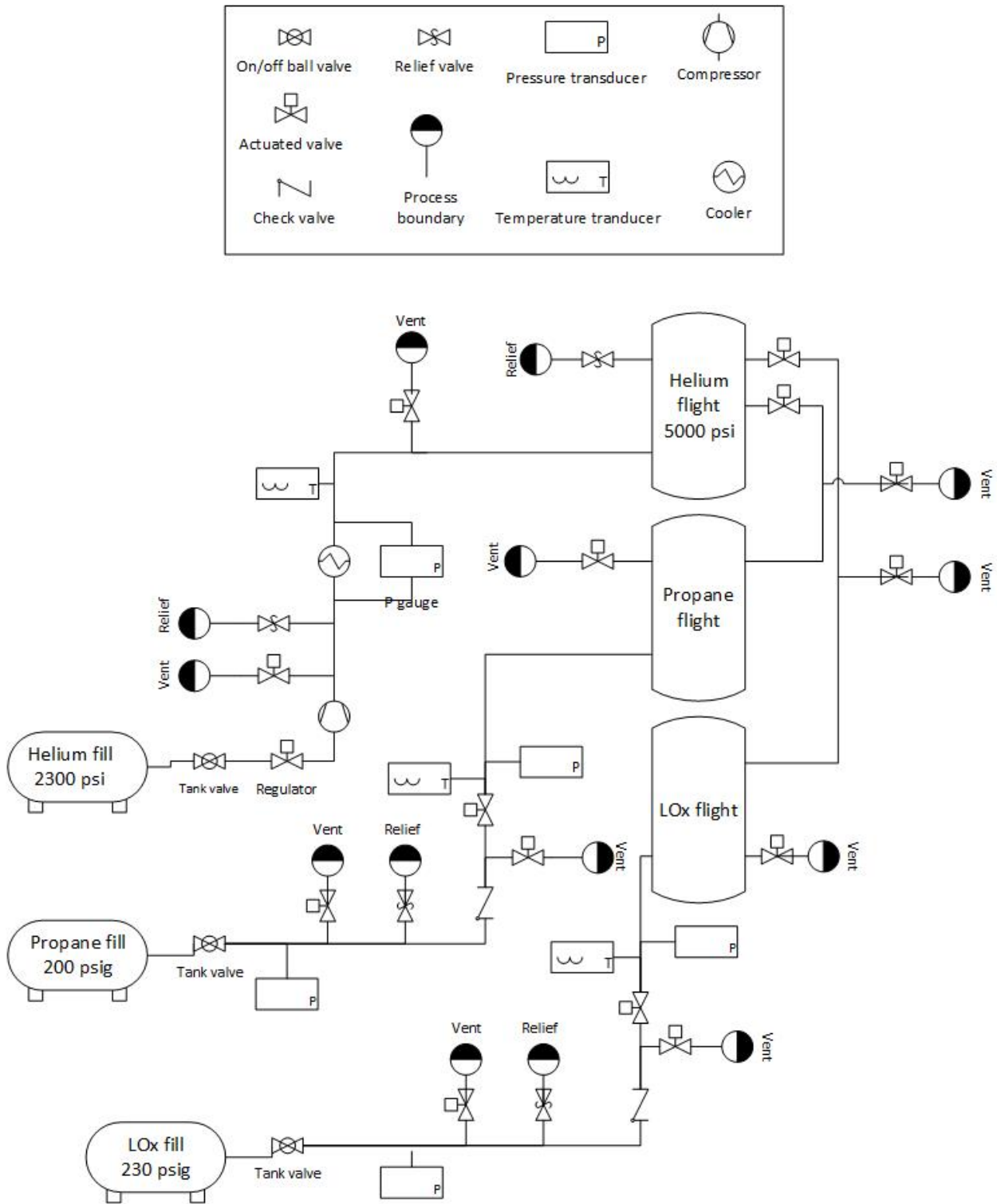
2. Fueling System

Figure 52   Fueling System Configuration

General Configuration

The tubing configuration required for fueling the rocket once it has been mounted onto the launch pad is illustrated in Figure 52. The propellants will be delivered onsite by suppliers as cryogenic liquids at the indicated pressures. The expected supplies needed are: a 250 L cylinder of LOX, and a 160 L cylinder of liquid propane. The helium will also be delivered onsite in a size 9 gas cylinder.

The tubing system from the fill tanks to the flight tanks are identical for both propellants. The dewars are expected to feature built-in valves that allow to control the inlet pressure to the cryogenic lines. Pressure transducers are incorporated to remotely monitor the pressure in each inlet tube, and pressure relief valves allow to avoid over-pressurization of the lines. The flight tanks are insulated with glass foam. They both feature permanent vents for boil-off of the cryogenic liquids, which are only closed moments before the launch of the rocket. Remotely actu-ated vent valves are incorporated between every closed space where cryogenic liquid could get trapped for safety purposes.

The interior of the cryogenic tubing system initially contains air at ambient temperature and pressure. Cryogenic liquid is released through the lines to cool them. The liquids will initially evaporate completely until the interior of the lines and the flight tanks reach the same temperature as the cryogenic liquids from the dewars. The vent in the flight tanks is sized properly to accommodate a 100 % boil-off rate of the fluids at this stage.

The tubing system from the helium fill tank to the flight tank is quite different. At an expected ambient temperature of 30 °C, the resulting pressure in the helium fill tank is around 2300 psi, as derived from the ideal gas law and specifications of size 9 gas cylinders for helium. However, the required pressure in the flight tank is 5000 psi. Hence, a compressor is incorporated into the tubing system of the helium. Furthermore, a cooler is subsequently used to reduce the temperature of the helium once it has been compressed, which allows to store it around ambient temperature on-board the rocket.

Inlet Pressure Determination for Propellants

The mass flow rate of the propellants $\dot{m}_{tube}$ to be achieved through their respective tubing systems is a function of their boil-off rate $\dot{m}_{vap}$ in the flight tanks, the final mass of propellant needed in each flight tank m_f, and the objective fill time T. The rate at which the tank fills is $\dot{m}_{fill} = \dot{m}_{tube} - \dot{m}_{vap}$. Setting $\dot{m}_{fill} = \frac{m_f}{T}$ and $\dot{m}_{tube} = \rho \dot{V}_{tube}$, we obtain

$$\dot{V}_{tube} = \frac{1}{\rho}\left[\frac{m_f}{T_{fill}} + \dot{m}_{vap}\right], \tag{1}$$

where ρ is the density of the respective fluid, assumed to be constant. Assuming a constant flow rate throughout the plumbing system, Equation 1 allows to find the volume flow required given a final propellant mass in the tank and an objective fill time, which will reasonably be between 45 and 60 minutes. The final masses of propellants required in the flight tanks takes into account the constant boil-off of the cryogenic fluids that will continue during preparations for launch after the fueling procedure is completed.

Given the volume flow rate to be achieved, the flow characteristics can be calculated. The diagram shown in Figure 52 intends to use tubing connections between 1 in. and 2 in. inside diameter. This assumption will be validated if the cryogenic lines operate at pressures and flow velocities that can be sustained by such tubes. The average flow velocity through the pipe at a given cross-section is $\bar{v} = \frac{\dot{V}_{tube}}{A}$, where $A = \frac{\pi D^2}{4}$ is the cross-sectional area of the tube, with D the inside diameter. The Reynold number $Re = \frac{\rho \bar{v} D}{\mu}$ can then be calculated, allowing to characterize laminar or turbulent flow in the pipe, where μ is the fluid's dynamic viscosity. A generally accepted value for laminar flow in circular pipes or tubes is $Re < 2300$ [8]. The estimated numbers for flow rate in the cryogenic tubes results in a Reynold number between 4000 and 9000, hence turbulent flow is assumed.

The governing equation for fully-developed, steady, turbulent, incompressible pipe flow, as derived from the energy equation of Reynold's Transport Theorem, gives [8]:

$$\left[\frac{p_1}{\rho_1} + \alpha_1\frac{\bar{v}_1^2}{2} + gz_1\right] - \left[\frac{p_2}{\rho_2} + \alpha_2\frac{\bar{v}_2^2}{2} + gz_2\right] = h_l + h_{lm}. \tag{2}$$

63

Index 1 refers to parameters at the upstream cross-section (fill tank inlet valve), and index 2 refers to parameters at the downstream cross-section (flight tank inlet). p is pressure; ρ is density; the kinetic energy coefficient α is a correction factor for turbulent flow which allows to use $\bar{v}$ in the energy equation; g is the gravitational constant; z is the height of the cross-section with respect to a reference point; $h_l = \frac{fL\bar{v}^2}{2D}$ is the energy loss due to pipe friction, where f is the Darcy friction factor obtained from experimental results and L is tubing length; and $h_{lm} = \frac{K\bar{v}^2}{2}$ is the energy loss due to fittings, valves, elbows, etc., with K being the loss coefficient determined experimentally for each situation.

We first verify the assumptions needed to use Equation 2. As they are in liquid phase, the cryogenic liquids are assumed to be incompressible. The flow has already been established to be turbulent, and such flow becomes fully-developed after 25 to 40 times the diameter of the entrance inlet, which resolves to between 25 in. and 80 in. for 1 in. to 2 in. diameter tubes. The plumbing lines are expected to measure around 50 ft in length each, hence the flow can be assumed to be fully-developed for the major part of the system. Finally, the flow is steady as no perturbations are applied to it during the fueling.

The independent parameter which must be solved for in Equation 2 is p_1, the required inlet pressure at the fill tank inlet valve. The other terms must hence be solved for in Equation 2. First, to find h_l the Darcy friction factor f is needed. For a specific tube given with surface roughness e, the Colebrook equation can be solved iteratively [8]:

$$\frac{1}{f} = -1.8 \log \left[\frac{e}{3.7D} + \frac{2.51}{Re\sqrt{f}} \right].$$

f is usually bounded by 0.008 and 0.1. Second, tabulated values of the loss coefficient K for different pipes, valves and fittings are available. These can be used in conjunction with the plumbing diagram in Figure 52 to solve for h_{lm}. Then, the height differential $z_2 - z_1$ is negligible, considering that the flight tanks will be positioned within 2 to 6 meters above the ground. Finally, the flow velocities $\bar{v}_1$ and $\bar{v}_2$ are identical. The kinetic energy coefficient approaches 1 throughout for turbulent flow, and the velocity term is negligible compared to the dominant terms in the equation. Hence, the kinetic energy term can be neglected.

The final expression for p_1 after manipulating Equation 2 is

$$p_1 = \rho \left[h_l + h_{lm} + \frac{p_2}{\rho} \right]. \tag{3}$$

Initial estimates lead to an inlet pressure of 40 psi for LOX and 25 psi for propane, which are readily achievable. These initial estimates are indicators, but the computations must be applied with more accurate numbers to obtain better results, notably after selecting the tubing lines, valves and fittings from designated suppliers.

Helium Tubing

The mass of helium needed to pressurize the two propellant tanks to around 1000 psi is determined from ideal gas law. The mass requirement of helium is expected to be between 5 and 10 kg. A size 9 pressurized helium gas cylinder is determined to contain around 20 kg of helium, from ideal gas relationships and the specifications of the tank.

As indicated in Figure 52, the pressure in the fill tank in launch conditions is expected to be around 2300 psi. Hence, a compressor able to achieve a pressure ratio of around 2.50 will be needed. The mass flow rate of helium required to power the compressor will be achieved with the regulator next to the helium fill tank valve. A cooler will be used to lower the temperature of the helium after its compression, such that it will be stored slightly above ambient temperature in the helium flight tank.

Propellant Pressurisation

Figure 52 shows two individual tubing connections between the helium and the propane and LOX flight tanks. Once the three flight tanks have been filled, the inlet valves are closed remotely and the lines are vented. Two individual tubing connections connect the helium flight tank to the two propellant tanks. As explained before, the propellants flow to the combustion chamber is pressure-fed. Once the fueling has been completed, before the launch of the rocket, the remotely actuated valves on these two tubing connections are opened. This allows the helium to flow from its 5000 psi tank to the propellant tanks and to pressurize them to around 1000 psi each.

O. Hazard Analysis

Please consult the table containing the Hazard Analysis attached to this report.

P. Risk Assessment

Please consult the table containing the Risk Assessment attached to this report.

Q. Payload

The payload shall consist of an experiment designed to measure the flux density of muons as a function of altitude and will have the goal to experimentally confirm the Pfozter curve. Previous experiments with muon detection have been carried out in planes and HABs, up to 120,000 ft[9][10], which showed an incomplete representation of possible data. 100 kilometers is ideal for this experiment because our detection will continuously record data points for the duration of the flight, and will create a much more complete representation of the data. While the payload will spend less total time in the atmosphere compared to other experiments, we still expect to collect sufficient data to characterize the Pfozter curve and determine the maximum, particularly during the (slower) descent phase.

The detector will be based on the Cosmic Watch detector developed by MIT[11], and will be optimised to collect as much data as possible in a small form factor. We also plan to distribute several detectors in the payload in order to maximise the sampling area. Furthermore, the detectors will be set up in a coincident mode, where one detector is placed directly above another which will serve to confirm a detection event. In addition, the detectors will need to be insulated and potentially have a heater to keep the detectors in optimal conditions (testing will need to be done in order to determine these optimal conditions). The form factor of the entire payload will be a 1-2U cubesat design, with a rough mass of 1-2 kg, depending on the size selected. As the experiment focuses on detectors, the weight will be kept to a minimum to focus the mass budget on other parts of the rocket.

The next steps involved with the development of the payload will include further research, designing, manufacturing and construction, testing, and finally implementing the payload into the rocket for launch. Specifically, the first steps will involve further research into the theoretical nature of the experiment, evaluating the materials that are appropriate and easily available, and procuring a design scheme to test and develop further. In addition, the detectors can be tuned to detect other types of particles which can allow us to modify the scope of the experiment, if we so choose.

III. Team Development

A. Succession Planning

Each critical role is expected to have multiple turnovers during the project timeline. It is crucial to minimize the amount of knowledge-loss accompanying each succession event and to ensure that no part of the project is neglected due to insufficient system-level oversight. The succession plan is broken down into four main parts:

1) Responsibility Distribution

2) Progressive Succession

3) On-boarding Periods

4) Knowledge Retention

These four strategies should aid in promoting a smooth transition of roles and responsibilities for all project-critical positions.

1. Responsibility Distribution

Effective distribution of responsibility provides an effective safety-net for ensuring continued operations. The overall goal is to increase the team's 'Bus Factor': the minimum number of personnel that would need to simultaneously stop working on the project (i.e. 'get hit by a bus') to cause mission-compromising difficulties. It is necessary for key personnel to be responsible for the overall project. Despite this, by breaking down the overarching objectives, we can

ensure that specific members are well-equipped to assume a project-level oversight role without the need to act as a supervisor for other projects. In this way, even with a turnover in a higher position, the sub-project leaders will ensure continuity of knowledge and of oversight during the transition period.

2. Progressive Succession

Progressive succession refers to ensuring that project leads represent the full spectrum of degree-pursuing students. Although this may sometimes lead to less prepared, lower year students being in lead roles, it will ultimately ensure that there are always at least some experienced members on the team. This must be implemented upon succession planning at the end of every school year to make sure that there is never a situation in which all critical roles are replaced in a single year.

3. On-Boarding Periods

It is important to have a soft transition of responsibilities and a gradual accommodation to a leadership role. This means deciding successors a couple months before the year ends and starting to introduce them to all aspects of the role at that point. We want members to enter a leadership role knowing exactly what will be expected from them throughout the year.

4. Knowledge Retention

As more alumni are accumulated, it is important for the team to maintain connection to graduated students for their advice and support. Although documentation and written knowledge retention is absolutely critical (see "Knowledge Retention"), it is also important to be able to ask a graduate member direct questions. The team has introduced Advisor positions where graduate members are kept in communication channels and consulted about issues. Additionally, written exit reports and transitional debriefings between role switches can greatly reduce transition time.

B. Knowledge Retention

The team has faced knowledge retention issues in the past, setting us back from progress that was made in previous years as experienced members left. This issue will be particularly highlighted on a multi-year project such as Base11, and concrete strategies have been developed to combat this. They are:

1) Local Documentation

2) Knowledge Accessibility

3) Body of Knowledge Files

1. Local Documentation

Local documentation refers to a "comment as you go" mentality from computer science; as files are created, code written and decisions made, a local paper trail is created as soon as possible. This approach requires that members frequently write out what they are doing and why they are doing it in a local location such as in the file they are working on itself. Examples of this include:

- Creating written explanations of what each subsystem in our SE diagram includes and excludes in order to remove ambiguity for future readers.
- Commenting code and software on the go instead of relying on the creators knowledge to make edits, knowledge that would disappear should the creator graduate.
- Taking minutes at meetings to document critical design/logistical decisions made, and the reasons for making them.
- Adding README.txt docs to subsystem folders containing CAD files elaborating any specifics about the CAD models.
- Generating detailed bills of materials for built projects, such that maintenance and upgrades will be easy in the future.

2. Knowledge Accessibility

Knowledge accessibility consists of two major components: ensuring future team members have physical/digital access to documentation and ensuring that current team members have access to the knowledge available to them.

Physical/digital accessibility involves a couple of key practices that when followed, ensure a complete transfer of files. Since to this point, the team had relied on Google drives to store and compile files for a given year, problems can arise from a lack of viewing/editing rights permitted by the file creator. The practice of ensuring that created files are set to be editable by all has been encouraged in the team, however with the amount of content created it is not always possible to enforce this. A more reliable method was implemented by purchase of a 2TB hard drive, onto which all data is periodically uploaded and archived. Lastly, a better platform than google drive can be used to store files, however that has not fully been explored.

Even if team members can physically view the information, that does not mean that it is in an accessible location for them to do so. Our strategy to handle this will be to create subteam specific reading lists, to enhance new team member on-boarding and to serve as a guiding resource during the year. A couple of such lists have already been created, with a directory to summarize resources.

3. Body of Knowledge (BoK) Files

The BoK files would be comprehensive knowledge documents that encompass all aspects of a given subteam or the team overall. Each subteam would have a formal, structured document and also a more informal, anecdotal document which would be used to convey word-of-mouth and spoken history knowledge that may not be encompassed in a structured setting. The documents per subteam would then be combined with a logistical/operation BoK document to form the overall McGill Rocket Team Body of Knowledge.

Three methods for knowledge transfer most effective for the team were identified:
1) Storytelling: the complementation of reports and formal documentation with the stories that surround them. In practice, this is the second, informal BoK document which the first formal BoK document would point to.
2) Process mapping: process used to identify users of knowledge as well as knowledge dispersion, by illustrating the internal processes of an organization (identifying decision makers, decision rationales, etc.). In practice, this process map outlines the structure of operation within the team, and in doing so sets the outline of the first BoK document.
3) After action reviews: documentation of lessons learned either throughout a project or after its completion. In practice, these start out as a set of notes from project team members and end up as a summary of the lessons learned, with the specifics contained in the notes.

A unified structure has not yet been finalized, although work on several parts of the full BoK has been started. For the technical aspect, the work done on our design-independent SE diagrams and layouts would serve as a key outline.

C. Outreach

The McGill Rocket Team hosted a tabling event at school in order to raise awareness about the team as well as educate students who are interested about rocketry about everything that the team does. This was a great opportunity to engage with the community at McGill University while increasing interest for students to join our team. During this event we also had the opportunity to film different team members speaking about their experiences and the work they have been doing. We intend to use this footage to create a promotional video which we can post online so members of the community can learn more about the team and our projects. In order to target women and underrepresented minorities we had 3 female students from different backgrounds represent the team at our tabling event. We aim to encourage diversity and female empowerment at all our events. We plan to continue doing tabling events in the future as we feel it is an efficient outreach method. An important tabling event will be in September when we will start recruiting for the 2019-2020 year. Next, in order to have a presence in the community, we will be starting an outreach program that targets CEGEP (pre-university) students in Montreal. We have been in contact with a physics teacher from John Abbott College who is involved with their outer space club at school. We would like to have these students come to McGill where members of our team can prepare a presentation and educate them on what the team does. As many CEGEP students end upcoming to McGill, our goal would be to encourage these students to join the team in their first year and then take on leadership roles in their later years. McGill has a shuttle that leaves from close to this CEGEP to our

downtown campus, which we would ideally be using in order to transport the kids. We believe that educating CEGEP students will be very beneficial as we are excited to inspire the younger generation and there are many passionate students who should be granted the opportunity to learn more about rocketry.

D. Business and Marketing

The first step of organising the business aspect of the Base11 project was to set forth our budget template which will be used over the next 2 years. Targeting the cohesion across our team's divisions and following some of our best accounting practices in recent years, we created an income statement template with an integrated yearly estimate by division as well as a general ledger giving us the ability to track every transaction. Every division will have their own budget sheet where they will make their estimates at the beginning of the fiscal year and fill out their expenses and incomes throughout the year. These inputs are linked to the McGill Rocket Team's income statement, where we will be able to see everyone's income and expenses separated by division. We found that on top of keeping track of our budget, it was important to assess and analyse our income throughout the competition in order to assess the accuracy of our estimates for the following year and to compare the expenses by division. We created integrated charts that are linked to the main income statement which will help us with this.

For fund-raising, the McGill Rocket Team launched a crowdfunding campaign from our house funding project Seeds of Change. We decided to use this channel over the likes of Kickstarter because it gave us the ability to double the donations during McGill24 day (March 13th) and because the channel gave us great exposure to McGill alumni who have been our main donors over the past years. 5 members of the McGill Rocket Team took initiative as coordinators of the project and attended seminars to make it as successful as possible. Based on previous crowdfunding experience with the team, we set out a target of $8,000. The campaign was launched the week of February 24th and our campaign promotional video followed. Not even a month in and we have surpassed $10,000 of funds raised. This has been a great success and we are planning on launching a similar campaign using the same channel the same time next year.

E. Sponsorship

In terms of sponsorship, we have identified and consolidated a comprehensive list of potential partners and sponsors, as well as all companies that currently sponsor the McGill Rocket Team or have sponsored us in the past. These companies are mostly concentrated in the Montreal region, but we have been looking into expanding our network into wider regions in the province. As of right now, we are only focusing our attention on developing new touchpoints with companies that are able to contribute cash sponsorships, since the McGill Rocket Team already maintains close relationships with companies that donate material sponsorships. In addition to this, we are redesigning the current sponsorship package to include Base11 specific information; once this is completed, we will begin to contact the companies from the aforementioned list of sponsors.

IV. Conclusion

Project Ariel is by far the most ambitious project that the McGill Rocket Team has attempted to undertake. While ultimately a tremendously rewarding experience for everyone involved, this project requires a lot of respect and careful planning. Our focus thus far has been to define as many systems as possible at a high level, to support the next steps of diving into project specifics. With a largely complete, solution-free systems architecture diagrams and several sub-systems entering the iterative stages of their development, there is a lot of work left to be done.

The next major area of focus will be realizing the logical systems in physical sub-systems and components. This would involve flushing out all system requirements, understanding necessary system performance under given conditions, and researching the teams ability to develop these components in-house. This would be the ultimate goal for the Critical Design Review in a year. Additionally, by far the best method to develop robust systems has been to continuously iterate over our designs. We need to come up with sub-systems that we believe will work, build them and subsequently break them through rigorous testing to see where we went wrong. The team mentality needs to be such that we do not get "Analysis Paralysis", where we are forever trying to reach the ideal design through thinking alone. A lot of our expected budgeting revolves around the fact that set-backs will happen, major components will fail or break, and we will have to restart sub-system development at potentially multiple points. Our goal is to dive into prototyping in concurrence with research and development, to get a feel for what is working and what is failing.

We have a very busy year ahead, and we are excited to bring our conceptual systems to reality.

V. Acknowledgments

References

[1] Dunn, B., "Fuel Table," , 1997. URL `https://yarchive.net/space/rocket/fuels/fuel_table.html`.

[2] Thuttle, J. L., "Perfect Bell Nozzle Parametric and Optimization Curves," , 1983.

[3] Beeson Harold, S. W., Smith Sarah, *Safe Use of Oxygen and Oxygen Systems: Handbook for Design, Operation, and Maintenance: 2nd Edition*, ASTM INTERNATIONAL, Standards, Worldwide, 2007.

[4] Rick Newlands, A. L., Martin Heywood, "Rocket vehicle loads and aiframe design," , 2016.

[5] Lessard, L., "Mechanics of Composites Materials Course Notes," , 2018.

[6] D. Igra, J. F., "Shock wave standoff distance for a sphere slightly above Mach one," *Shock Waves*, Vol. 20, No. 5, 2010, p. 444. doi:10.1007/s00193-010-0273-z.

[7] Barrowman, J., "The Practical Calculation of the Aerodynamic Characteristics of Slender Finned Vehicles," Master's thesis, The Catholic University of America, 3 1967.

[8] Phillip J. Pritchard, J. W. M., *Introduction to Fluid Mechanics, 9th Edition*, Fox and McDonald's, 2014.

[9] Rodriguez, J., "Smoky Mountain Cosmic Ray Flux Altitude Study," , 2013. URL `https://www.i2u2.org/elab/cosmic/posters/display.jsp?type=paper&name=smokey_mountain_cosmic_ray_flux_altitude_study.data`.

[10] HACR, W. T., "West Virginia University High Altitude Cosmic Radiation (HACR) Detector Payload Summary and Flight Science Report," Master's thesis, West Virginia University, West Virginia University, Morgantown, WV 26506/6106, 12 2007.

[11] Frankiewicz, P. P. . K., "Cosmic Watch," , 2017. URL `http://cosmicwatch.lns.mit.edu/`.

Figure 53　Team Fish Bertrand